European Journal of Medicinal Chemistry 54 (2012) 447–462

Contents lists available at SciVerse ScienceDirect

European Journal of Medicinal Chemistry

journal homepage: http://www.elsevier.com/locate/ejmech

Original article

Benzothiazoles: Search for anticancer agents

Malleshappa N. Noolvi [a,*], Harun M. Patel [b], Manpreet Kaur [c]

[a] Department of Pharmaceutical Chemistry, Shree Dhanvantary Pharmacy College, Kim (Surat)-3941110, Gujrat, India
[b] Department of Pharmaceutical Chemistry, R.C. Patel Institute of Pharmaceutical Education and Research, Shirpur (Dhule)-425405, Maharashtra, India
[c] Department of Pharmaceutical Chemistry, ASBASJSM College of Pharmacy, Bela (Ropar)-140111, Punjab, India

HIGHLIGHTS

- Synthesis and *in vitro* anticancer activity of a novel 2-amino benzothiazoles.
- Characterized by IR, ^{1}H NMR, ^{13}C NMR, and HRMS technique.
- The title compound **4e** shown promising anti-tumor activity.

GRAPHICAL ABSTRACT

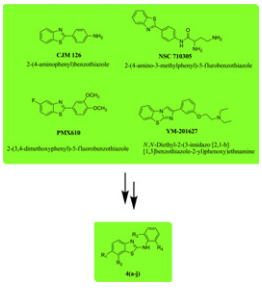

ARTICLE INFO

Article history:
Received 25 January 2012
Received in revised form
16 May 2012
Accepted 22 May 2012
Available online 30 May 2012

Keywords:
Synthesis 2-amino benzothiazoles
Antitumor
Pharmacophore mapping
Docking

ABSTRACT

Novel derivatives of 2-amino benzothiazoles **4(a–j)** have been synthesized and tested for their antitumor activity using National Cancer Institute (NCI) disease oriented antitumor screen protocol against nine panel of cancer cell lines. Among the synthesized compounds, two compounds were granted NSC code and screened at National Cancer Institute (NCI)-USA for anticancer activity at a single high dose (10^{-5} M) and five dose in full NCI 60 cell panel. Among the selected compounds ,7-chloro-*N*-(2,6-dichlorophenyl) benzo[*d*]thiazol-2-amine (**4i**) with GI_{50} values of 7.18×10^{-8} M against Non-Small Cell HOP-92 Lung Cancer cell line proved to be the most active members in this study. Virtual screening was carried out through docking the designed compounds into the ATP binding site of epidermal growth factor receptor (EGFR) to predict if these compounds have analogous binding mode to the EGFR inhibitors.

1. Introduction

Nowadays, health is one of the most important domains which we human beings have focused on in our society. However, tumor is the biggest killer of our lives, so there has been steadily increasing research in the field of anticancer therapy over recent years. With the current chemotherapy, lack of selectivity of chemotherapeutic agents against cancerous cells is a significant problem. Receptor tyrosine kinases (RTKs) are high affinity cell surface receptors that bind polypeptide growth factors, cytokines and hormones. They have been shown to be key regulators of normal cellular processes and additionally play a critical role in the development and progression of many types of cancer [1]. Protein tyrosine kinases occupy a central position in the control of cellular proliferation. Over expression of certain RTKs show association with promotion and maintenance of malignancies. For example, the epidermal growth factor (EGF) receptor tyrosine kinases of the erbB family (which includes erbB1–erbB4) is frequently expressed at high levels in certain carcinomas and shows an inverse correlation with survival (particularly breast, colon and bladder cancers) [2]. Thus, inactivation of the specific tyrosine kinases those are responsible for the malignant phenotype of certain cancers represent a potential approach for design of antiproliferative drugs [3].

* Corresponding author. Tel.: +91 9417563874; fax: +91 1881263655.
E-mail address: mnoolvi@yahoo.co.uk (M.N. Noolvi).

0223-5234/$ – see front matter © 2012 Elsevier Masson SAS. All rights reserved.
doi:10.1016/j.ejmech.2012.05.028

Benzothiazole type compounds have attracted considerable attention to anticancer research [4–14], and several attempts were made for modifying the benzothiazole nucleus to improve their antitumor activities. Modifications on the benzothiazole nucleus have resulted in a large number of compounds having diverse pharmacological activities. Among them imidazo benzothiazoles as well as polymerized benzothiazoles and other substituted benzothiazoles such as 2-(3,4-dimethoxyphenyl)-5-fluorobenzothiazole (PMX 610) (Fig. 1) has been shown to exhibit exquisitely potent ($GI_{50} < 0.1$ nM) and selective *in vitro* antitumor properties in human cancer cell lines (e.g., colon, non small – cell lung and breast subpanels) of the National Cancer Institute (NCI) 60 human cancer cell line screen [15] and also exhibited remarkable antitumor activity against malignant cell lines [16]. 2-(4-aminophenyl)-benzothiazole (CJM 126) and its analogs comprise a novel mechanistic class of antitumor agents [17,18]. These nucleuses come from the related structure polyhydroxylated 2-phenylbenzothiazoles, flavone quercetin and the isoflavone genistein, which are tyrosine kinase inhibitors bearing potent antitumor activity [19,20]. The isoflavone, genistein [21] and the flavone, quercetin [22] are competitive inhibitors at the ATP-binding site of kinases [23,24]. As the crystal structure of 5,6-dimethoxy-2-(4-methoxyphenyl)benzothiazole was solved [20], the preliminary analysis based on comparisons between polyhydroxylated 2-phenylbenzothiazoles and the adenine fragment of ATP suggested that suitably substituted benzothiazoles might mimic the ATP competitive binding of genistein and quercetin at tyrosine kinases.

Hence in continuation of our efforts on the design and synthesis of novel anti-cancer agents [25–29] and keeping in mind the medicinal importance of benzothiazole moiety, we synthesized and *in vitro* evaluated benzothiazoles at National Cancer Institute (NCI-USA) for anti-tumor activity. We have also tried to dock the synthesized compounds with the crystal structure of EGFR to explore the possible anticancer mechanism of our compounds. Prior compounds have been reported [30,31] to compare the anticancer activity of such compounds.

2. Rational and design

Benzothiazoles act via competing with ATP for binding at the catalytic domain of tyrosine kinase [20]. The ATP binding site has the following features; Adenine region – contains two key Hydrogen bonds formed by the interaction of N-1 and N-6 amino group of the adenine ring. Many potent inhibitors use one of these Hydrogen bonds. Sugar region – a hydrophilic region, except a few e.g. EGFR. Hydrophobic pocket – though not used by ATP but plays an important role in inhibitor selectivity. Hydrophobic channels – it is not used by ATP and may be exploited for inhibitor specificity. Phosphate binding region – This is used for improving inhibitor selectivity [32].

In this study, we present a new sub-family of compounds containing 2-anilino benzothiazole core as EGFR inhibitors. Our strategy is directed toward designing a variety of ligands which are structurally similar with basic skeleton, 4-anilino quinazoline of tinibs (erlotinib, lapatinib, gefitinib and canaratinib) with diverse chemical properties (Fig. 2). We replaced quinazoline ring with benzothiazole since both are isosteric with adenine portion of ATP

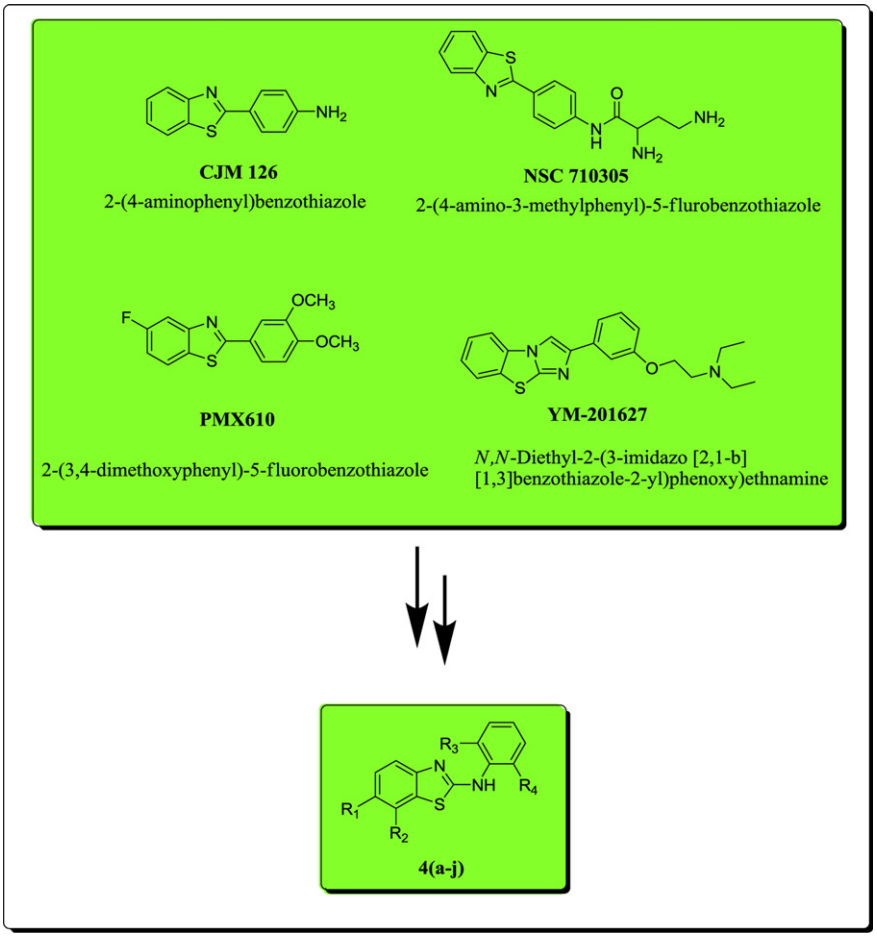

Fig. 1. Reported and proposed antitumor benzothiazole derivatives.

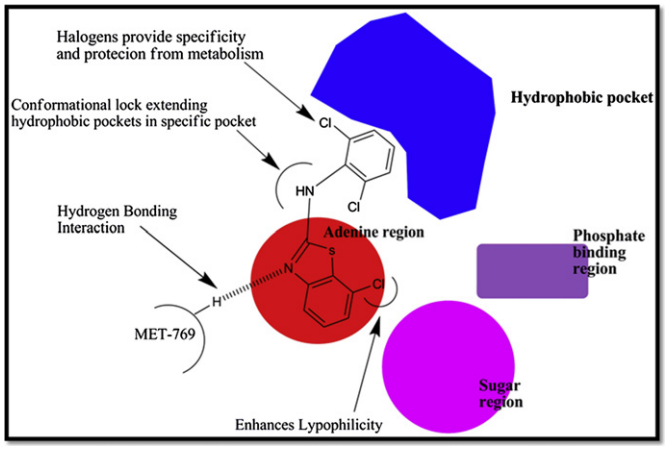

Fig. 2. Proposed hypothetical model of the highly active 7-chloro-*N*-(2,6-dichlorophenyl)benzo[*d*]thiazol-2-amine (**4i**) bound to ATP binding site of EGFR protein tyrosine kinase.

and can mimic the ATP competitive binding regions of EGFR tyrosine kinase. Like 4-aniline group in tinibs (erlotinib, lapatinib, gefitinib and canaratinib) we introduced substituted aniline ring at 2nd position of benzothiazole since secondary amino group at 2nd position of benzothiazoles is acting as conformational lock and extending substituted aniline portion into the hydrophobic pockets of EGFR – tyrosine kinase, making predominantly hydrophobic interactions with the protein mimicking the 3′-chloro-4′-[(3-fluorobenzyl) oxy] aniline group of lapatinib (Fig. 3). We put both electron withdrawing (Cl) and electron donating (CH_3) anilines at 2nd position just to check the effect of these substituents over anticancer activity since it is well known that presence of electron withdrawing group on anilines provides protection from metabolism and provides specificity to the molecules.

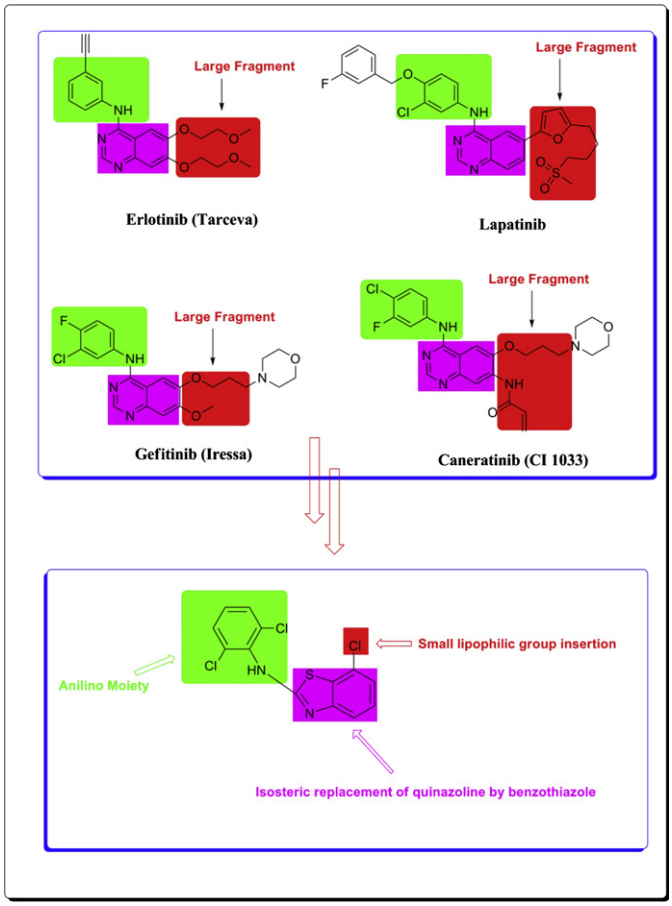

Fig. 3. Rational designing of proposed compounds based upon known EGFR-Tyrosine kinase inhibitor.

3. Chemistry

In Scheme 1 the compounds were synthesized using various isothiocyanates **2(a–e)**, which was prepared from different aromatic primary amines **1(a–e)** [33]. Prepared isothiocyanates **2(a–e)** yielded thioureas **3 (a–e)** on condensation with 2,6-dimethyl and 2,6-dichloro aniline [25]. Oxidative cyclization of **3 (a–e)** by bromine resulted in the synthesis of proposed compounds **4 (a–j)**. Physical data of the synthesized compound is given in Table 1.

The derivatives were characterized by spectral studies using IR, ^{1}H NMR, ^{13}C NMR and HRMS. The structures of thiocynates were confirmed through the following spectral data **2 (a–e)**. IR absorption peak at ~2200-2000 cm^{-1} corresponding to – SCN and ^{1}H NMR showing a ~δ 6.80–7.90 ppm for aromatic protons of isothiocyanates **2 (a–e)**. Thioureas **3 (a–j)** were confirmed by the absence of characteristic IR absorption peak at ~2200–2000 cm^{-1}

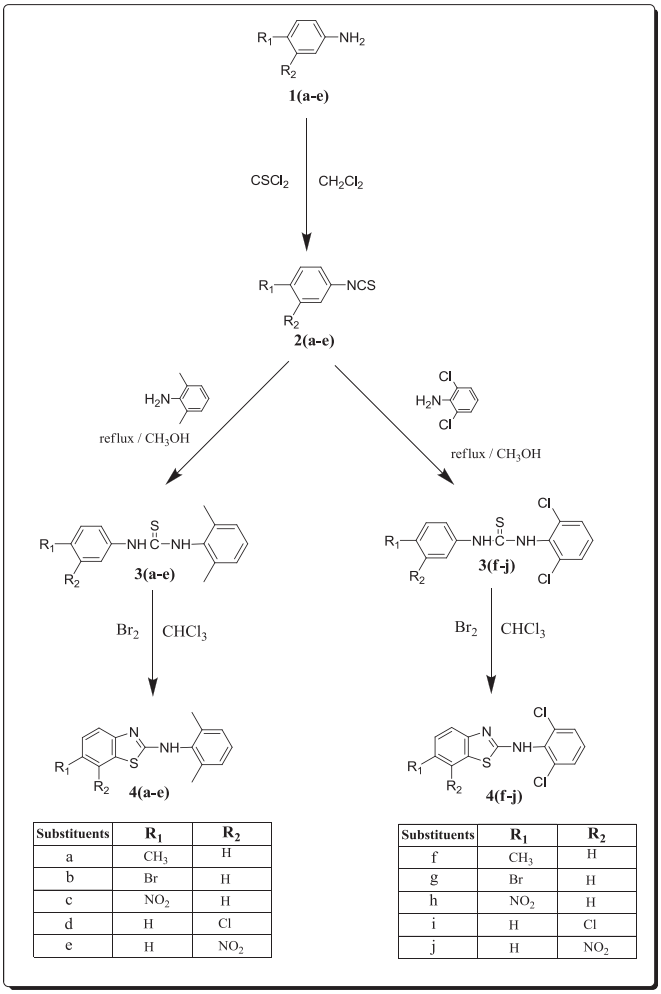

Substituents	R_1	R_2
a	CH_3	H
b	Br	H
c	NO_2	H
d	H	Cl
e	H	NO_2

Substituents	R_1	R_2
f	CH_3	H
g	Br	H
h	NO_2	H
i	H	Cl
j	H	NO_2

Scheme 1.

of – SCN group. Bands at ~1610–1600 cm^{-1} confirmed formation of thioureas –NH–CS–NH–. Further occurrence of two broad peaks at ~δ 9.23 and 8.14 ppm corresponding two – NH groups substantiated the formation of thioureas. ^{13}C NMR confirmed conversion of – SCN to–NH–CS–NH– by a peak at ~δ 181–179 ppm corresponding to >C═S. The novel 2-amino benzothiazoles **4 (a–j)** showed IR absorption band at ~3300 (NH-strech), ~3000 (CH-strech), ~1600 (NH-bend) and ~700 (C–Cl) cm^{-1}. ^1H NMR spectra revealed all the corresponding peaks at ~δ 2.30 ppm for $-CH_3$, ~δ 4.50 for –NH– and ~δ 6.76–8.23 ppm for aromatic protons. ^{13}C NMR gave valuable information to confirm cyclisation of substituted thioureas to respective substituted 2-amino benzothiazoles with characteristic peak at ~δ 172 ppm for C-2. Further HRMS gave all the molecular ion peaks corresponding to molecular weight of confirmed novel compounds.

4. Pharmacology

The *in vitro* anticancer screening at NCI is a two-stage process, beginning with the evaluation of all compounds against the 60 cell lines at a single dose of 10 μM. The output from the single dose screen is reported as a mean graph and is available for analysis by the COMPARE program. Compounds which exhibit significant growth inhibition are evaluated against the 60 cell panel at five concentration levels. The human tumor cell lines of the cancer screening panel are grown in RPMI 1640 medium containing 5% fetal bovine serum and 2 mM L-glutamine. For a typical screening experiment, cells are inoculated into 96 well microtiter plates in 100 μL at plating densities ranging from 5000 to 40,000 cells/well depending on the doubling time of individual cell lines. After cell inoculation, the microtiter plates are incubated at 37 °C, 5% CO_2,

Table 1
Physicochemical properties of the synthesized compounds **4(a–j)**.

No.	Compounds	NSC code	Molecular formula	Melting point (°C)	Percentage yield (%)
4a	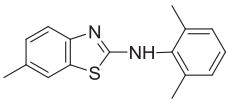	105624/759789	$C_{16}H_{16}N_2S$	146-148	32
4b	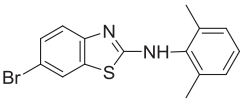	–	$C_{15}H_{13}BrN_2S$	156-160	28
4c	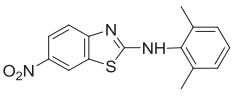	–	$C_{15}H_{13}N_3O_2S$	162-166	41
4d	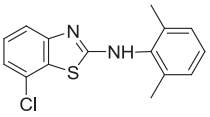	–	$C_{15}H_{13}ClN_2S$	128-134	23
4e	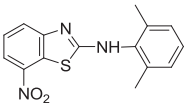	–	$C_{15}H_{13}N_3O_2S$	124-128	30
4f	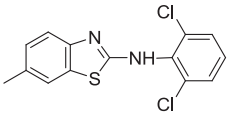	–	$C_{14}H_{10}C_{l2}N_2S$	138-142	38
4g	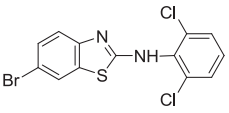	–	$C_{13}H_7BrCl_2N_2S$	122-125	42
4h	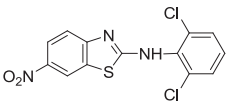	–	$C_{13}H_7Cl_2N_3O_2S$	172-174	44
4i	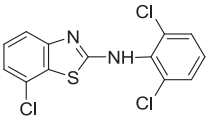	105628/759790	$C_{13}H_7Cl_3N_2S$	165-168	31
4j	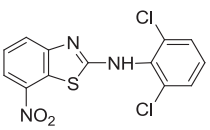	–	$C_{13}H_7Cl_2N_3O_2S$	152-156	34

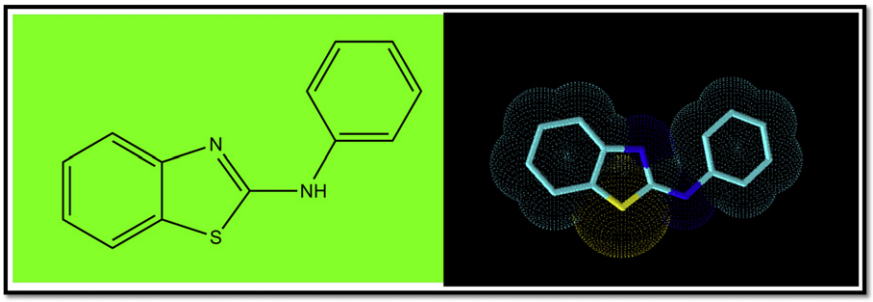

Fig. 4. 2D and 3D view of 2-anilino benzothiazole template used for pharmacophoric mapping alignment.

95% air and 100% relative humidity for 24 h prior to addition of experimental drugs.

After 24 h, two plates of each cell line are fixed *in situ* with TCA, to represent a measurement of the cell population for each cell line at the time of drug addition (Tz). Experimental drugs are solubilized in dimethyl sulfoxide at 400 fold the desired final maximum test concentration and stored frozen prior to use. At the time of drug addition, an aliquot of frozen concentrate is thawed and diluted to twice the desired final maximum test concentration with complete medium containing 50 μg/ml gentamicin. Additional four, 10-fold or ½ log serial dilutions are made to provide a total of five drug concentrations plus control. Aliquots of 100 μL of these different drug dilutions are added to the appropriate microtiter wells already containing 100 μL of medium, resulting in the required final drug concentrations.

Following drug addition, the plates are incubated for an additional 48 h at 37 °C, 5% CO_2, 95% air, and 100% relative humidity. For adherent cells, the assay is terminated by the addition of cold TCA. Cells are fixed *in situ* by the gentle addition of 50 μL of cold 50% (w/v) TCA (final concentration, 10% TCA) and incubated for 60 min at 4 °C. The supernatant is discarded, and the plates are washed five times with tap water and air dried. Sulforhodamine B (SRB) solution (100 μl) at 0.4% (w/v) in 1% acetic acid is added to each well, and plates are incubated for 10 min at room temperature. After staining, unbound dye is removed by washing five times with 1% acetic acid and the plates are air dried. Bound stain is subsequently solubilized with 10 mM trizma base, and the absorbance is read on an automated plate reader at a wavelength of 515 nm. For suspension cells, the methodology is the same except that the assay is terminated by fixing settled cells at the bottom of the wells by gently adding 50 μL of 80% TCA (final concentration, 16% TCA). Using the seven absorbance measurements [time zero, (Tz), control growth, (C), and test growth in the presence of drug at the five concentration levels (Ti)], the percentage growth is calculated at each of the drug concentrations levels. Percentage growth inhibition is calculated as:

$$[(\mathrm{Ti}-\mathrm{Tz})/(\mathrm{C}-\mathrm{Tz})]\times 100 \text{ for concentrations for which } \mathrm{Ti} >/= \mathrm{Tz}$$

$$[(\mathrm{Ti}-\mathrm{Tz})/\mathrm{Tz}]\times 100 \text{ for concentrations for which } \mathrm{Ti} < \mathrm{Tz}.$$

Three dose response parameters are calculated for each experimental agent. Growth inhibition of 50% (GI_{50}) is calculated from [(Ti−Tz)/(C−Tz)] × 100 = 50, which is the drug concentration resulting in a 50% reduction in the net protein increase (as measured by SRB staining) in control cells during the drug incubation. The drug concentration resulting in total growth inhibition (TGI) is calculated from Ti = Tz. The LC_{50} (concentration of drug resulting in a 50% reduction in the measured protein at the end of the drug treatment as compared to that at the beginning) indicating

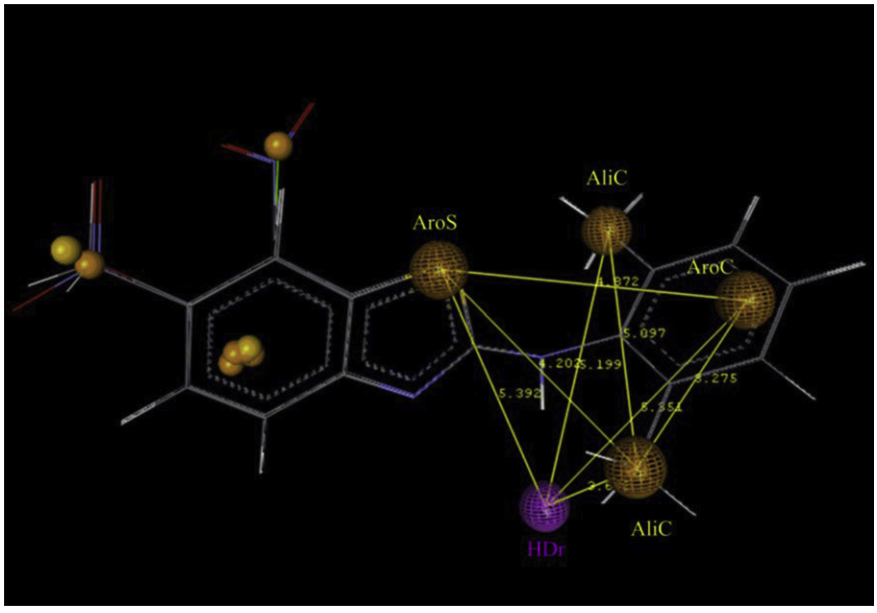

Fig. 5. Common biopharmacophore of **4(a–j)**.

a net loss of cells following treatment is calculated from [(Ti−Tz)/Tz] × 100 = −50. Values are calculated for each of these three parameters if the level of activity is reached; however, if the effect is not reached or is exceeded, the value for that parameter is expressed as greater or less than the maximum or minimum concentration tested [34–36].

5. Pharmacophore mapping

A pharmacophore is the ensemble of steric and electronic features that is necessary to ensure the optimal supramolecular interactions with a specific biological targets and to trigger (or to block) its biological response. 3D pharmacophore modeling is

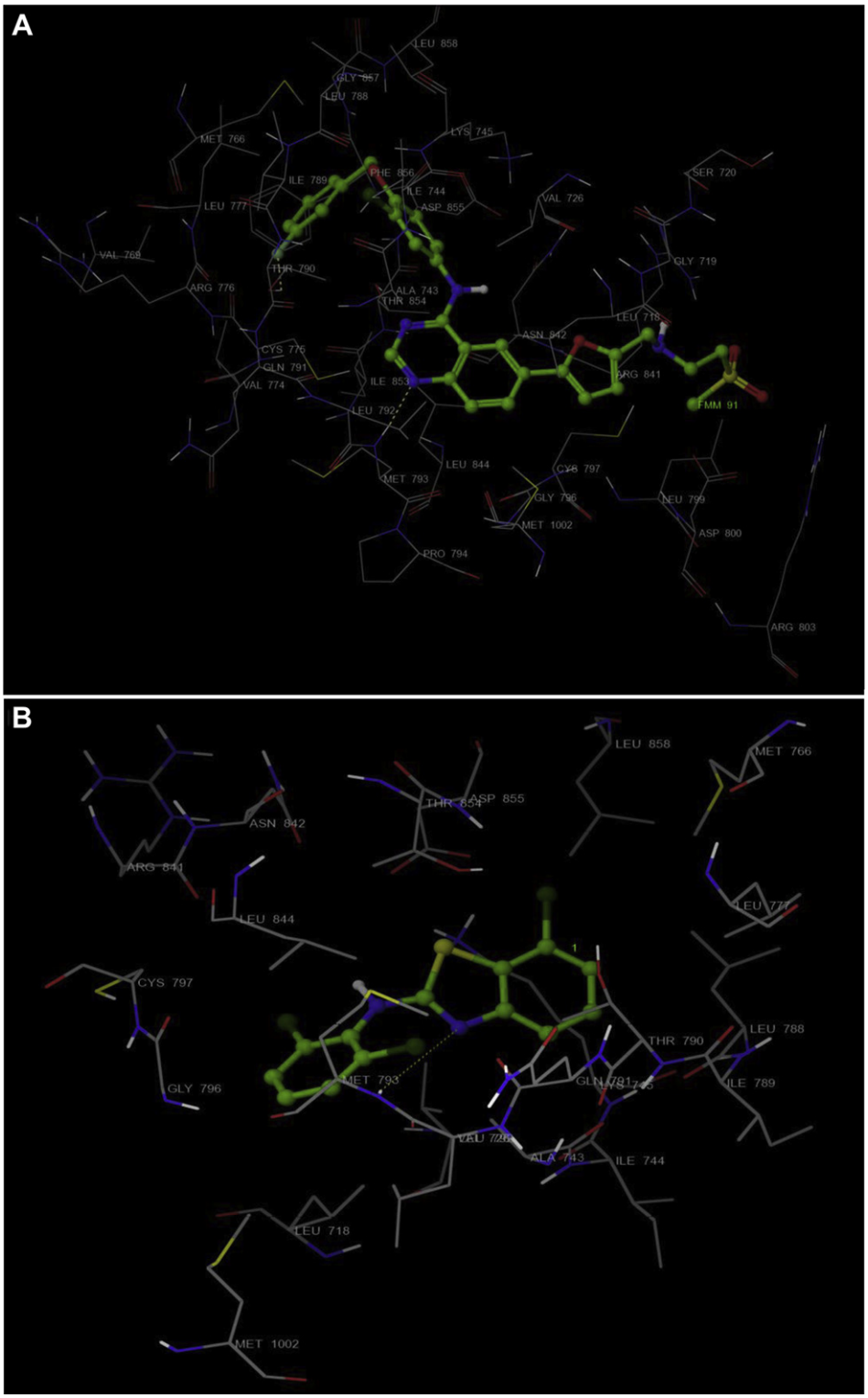

Fig. 6. Binding mode of **Lapatinib** (**A**) and compound **4i** (**B**) in the ATP binding site of EGFR-TK showing H bonds between N-1 of quinazoline (**Lapatinib**) and N-3 of benzothiazole (**4i**) with Met 793.

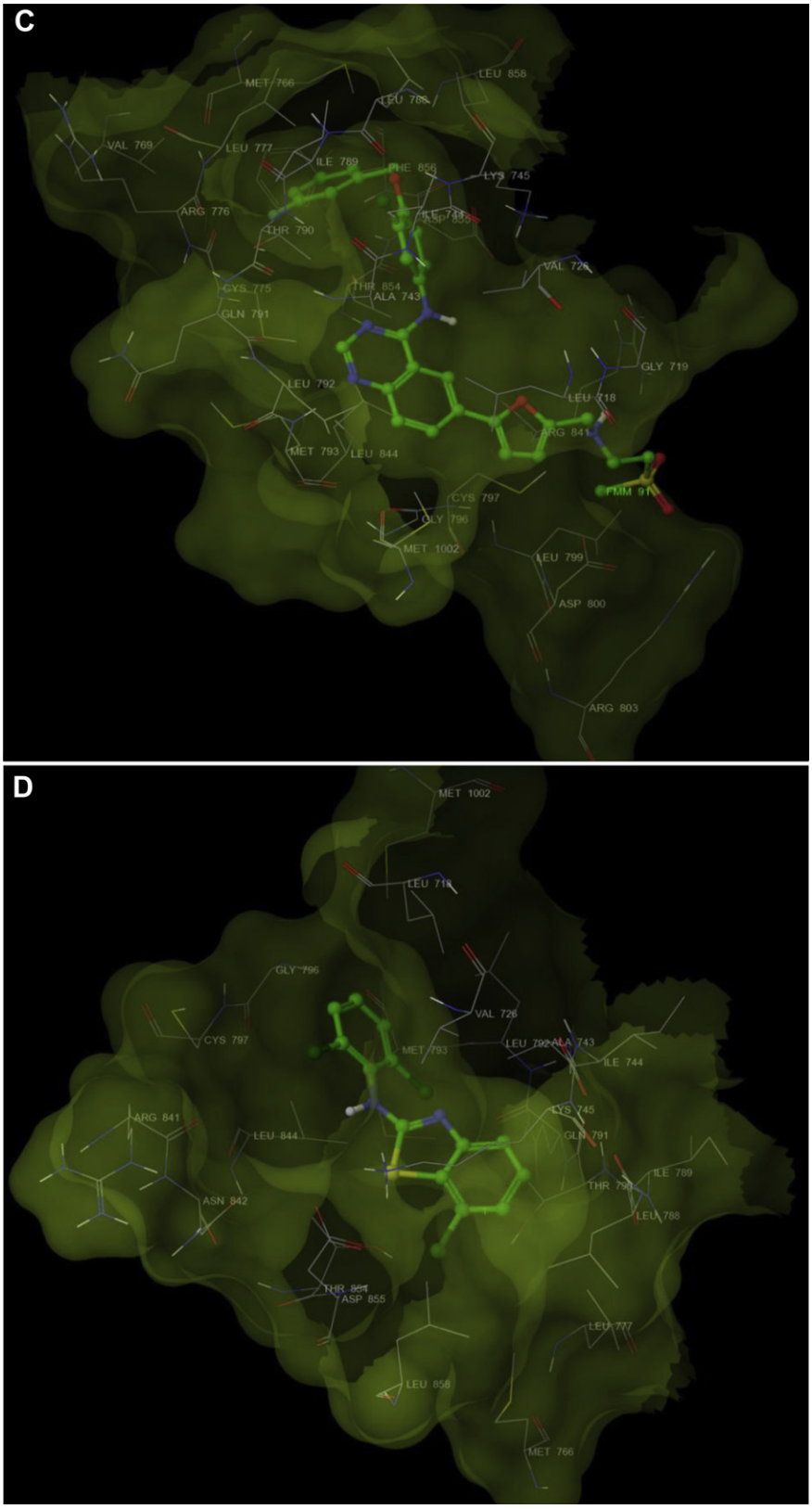

Fig. 7. Binding mode of **Lapatinib** (**C**) and compound **4i** (**D**) in the ATP binding site of EGFR-TK showing residue within 5 Å.

Table 2
Glide docking results based on hydrophobic interaction, hydrogen bonding interaction, glide dock score, E-model and good Vdw-interaction.

No.	Compounds	Hydrophobic interaction (within 5 Å)	H-bond interaction	Glide score (kcal/mol)	E-model	Good Vdw -interaction
4a	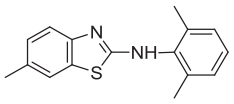	ALA-743, ARG-841, ASP-855, CYS-797, GLY-791, GLY-796, ILE-744, LEU-718, LEU-777, LEU-788, LEU-792, LEU-844, LEU-858, LYS-745, MET-1002, MET-766, MET-793, PHE-856, PRO-794, THR-790, THR-854, VAL-726, PHE-795, VAL-845	N- of benzothiazole and H atom of amino acid backbone of MET-793	−7.85	−70.781	221
4b	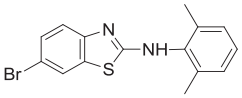	ALA-743, ARG-776, ARG-841, ASN-842, ASP-855, CYS-775, CYS-797, GLN-791, GLY-857, LEU-718, LEU-777, LEU-788, LEU-792, LEU-844, LEU-858, LYS-745, MET-766, PHE-856, THR-790, VAL-726, VAL-774, LEU-795, VAL-845	N- of benzothiazole and H atom of amino acid backbone of MET-793	−8.23	−80.710	234
4c	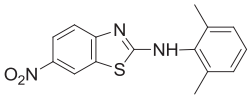	ALA-743, ARG-841, ASN-842, ASP-855, CYS-775, CYS-797, GLY-796, GLY-857, LEU-718, LEU-777, LEU-788, LEU-858, LYS-745, MET-766, PHE-856, THR-790, THR-854, VAL-726, VAL-769, LEU-778	N- of benzothiazole and H atom of amino acid backbone of MET-793	−8.48	−85.15	268
4d	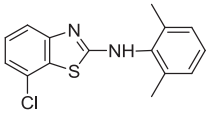	ALA-743, ARG-841, ASN-842, ASP-855, CYS-797, GLY-796, ILE-744, ILE-789, LEU-718, LEU-777, LEU-788, LEU-792, LEU-844, LYS-745, MET-1002, MET-766, MET-793, THR-790, THR-854, VAL-726, VAL-774, GLY-721, TYR-727, VAL-843	N- of benzothiazole and H atom of amino acid backbone of MET-793	−8.44	−95.56	198
4e	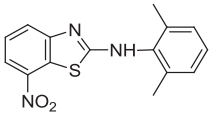	ALA-743, ARG-841, ASN-842, ASP-855, CYS-797, GLY-796, ILE-744, ILE-789, LEU-718, LEU-777, LEU-788, LEU-792, LEU-844, LYS-745, MET-1002, MET-766, MET-793, PHE-856, THR-790, THR-854, VAL-720, VAL-843, GLY-721, TYR-727	N- of benzothiazole and H atom of amino acid backbone of MET-793 N- of Nitro group and H atom of amino acid backbone of ASP-855	−8.80	−89.86	298
4f	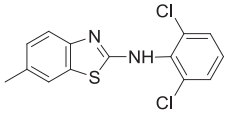	ALA-743, ARG-841, ASN-842, ASP-855, CYS-797, GLY-719, GLY-796, ILE-744, ILE-789, LEU-718, LEU-777, LEU-788, LEU-792, LEU-844, LYS-745, MET-1002, MET-766, MET-793, SER-720, THR-790, THR-854, VAL-726, LEU-778, GLY-721	N- of benzothiazole and H atom of amino acid backbone of MET-793	−8.94	−74.92	231
4g	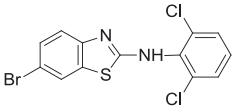	ALA-743, ARG-776, ARG-841, ASN-842, ASP-885, CYS-775, CYS-797, GLY-857, LEU-718, LEU-788, LEU-792, MET-766, MET-793, PHE-856, THR-790, THR-854, VAL-726, VAL-769, VAL-774, LYS-745	N- of benzothiazole and H atom of amino acid backbone of MET-793	−8.68	−71.03	282
4h	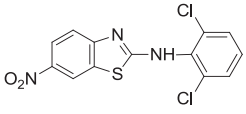	ALA-743, ARG-841, ASN-842, ASP-855, CYS-797, GLY-719, ILE-744, ILE-789, LEU-718, LEU-777, LEU-788, LEU-844, LYS-745, MET-1002, SER-720, THR-790, THR-854, VAL-720, GLY-721	N- of benzothiazole and H atom of amino acid backbone of MET-793	−8.48	−79.45	221
4i	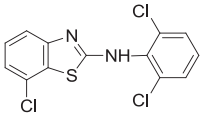	ALA-743, ARG-841, ASP-855, CYS-797, GLN-791, ILE-744, ILE-789, LEU-718, LEU-777, LEU-788, LEU-844, LYS-745, MET-1002, MET-766, MET-793, THR-790, THR-854, VAL-726, LEU-758, GLY-797, TYR-727	N- of benzothiazole and H atom of amino acid backbone of MET-793	−9.95	−98.16	301
4j	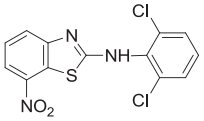	ALA-743, ARG-841, ASN-842, ASP-855, CYS-797, GLY-719, LEU-718, LEU-771, LEU-792, LEU-842, LYS-745, MET-766, MET-793, PHE-856, THR-854, ILE-789, GLY-721, ILE-744	N- of benzothiazole and H atom of amino acid backbone of MET-793 N- of Nitro group and H atom of amino acid backbone of ASP-855	−9.49	−92.18	254

a technique for designing the interaction of a small molecule ligand with a macromolecular target. Vlife MDS MolSign module is used for the identification, generation and analysis of pharmacophore by aligning small organic molecules based on their pharmacophore features using PLS method [37].

A pharmacophore can be derived in a ligand-based manner, by flexibility overlaying a set of active molecules and determining those conformations that are able to be overlaid in such a way that a maximum number of important chemical features geometrically overlap. To be a useful tool for drug design, a pharmacophore model

has to provide valid information for medicinal chemist investigating structure-activity relationship. The pharmacophore model has to describe the nature of the functional groups involved in ligand-target interactions, as well as the type of the non-covalent bonding and interchange distances.

All the structures of the compounds were drawn in 2D-APPL mode of software and exported to 3D. Three-dimensional structures of all compounds have been constructed using MDS 3.5 version of Vlife science and their geometries were subsequently optimized to make the conformations having least potential energy. Energy minimizations were performed using Merck molecular force field (MMFF) and MMFF charge [38] followed by considering distance-dependent dielectric constant of 1.0 and convergence criterion of 0.01 kcal/mol. The compounds were then subjected to conformational analysis using Montecarlo conformational search with RMS gradient of 0.001 kcal/mol using a MMFF force field. Molecular alignment is a crucial step for pharmacophoric study to obtain meaningful results. This method is based on moving of molecules in 3D space, which is related to the conformational flexibility of molecules. The goal is to obtain optimal alignment between the molecular structures [39]. All molecules in the data set were aligned by template-based method using 2-anilino benzothiazole as template, where a template is built by considering common substructures in the series as shown in Fig. 4. A highly bioactive energetically stable conformation in this class of compounds is chosen as a reference molecule on which other molecules in the data set are aligned, considering template as a basis for the alignment. All the synthesized molecules were taken for pharmacophore development. Highly active molecule to set as reference. The reference molecule is the molecule on which other molecules of the aligned data set get aligned. For pharmacophoric identification tolerance limit and maximum distance allowed between two features were set up to 10 Å. This abstract model containing chemical functionalities such as hydrogen bond donor,

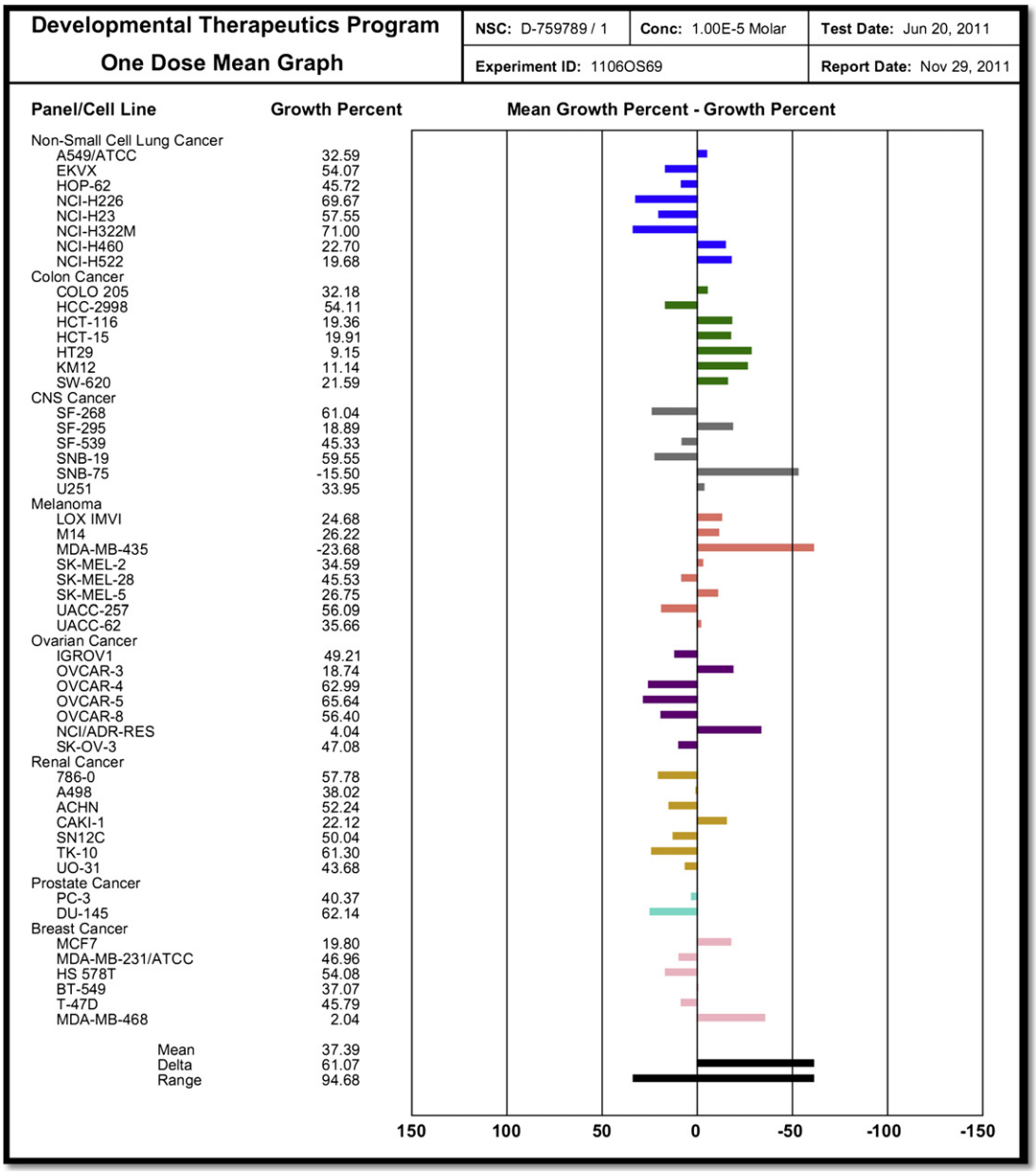

Fig. 8. Single dose assay of compound **4a** (NSC: 105624/759789).

hydrogen bond acceptor and aromatic carbon center, can serve as an effective search filter.

6. Docking study

The molecular docking tool, GLIDE (Schordinger Inc., USA) (2006) was used for ligand docking studies into tyrosine kinase receptor binding pocket. The crystal structures of tyrosine kinase was obtained from protein data bank (PDB ID: 1XKK) [40]. The protein preparation was carried out using 'protein preparation wizard' in Maestro 9.0 in two steps, preparation and refinement. After ensuring chemical correctness, water molecules in the crystal structures were deleted and hydrogens were added, where they were missing. Using the OPLS 2005 force field energy of crystal structure was minimized [41]. Grids were defined centering them on the ligand in the crystal structure using the default box size. The ligands were built using maestro build panel and prepared by Ligprep 2.2 module which produce the low energy conformer of

National Cancer Institute Developmental Therapeutics Program
In-Vitro Testing Results

NSC : D - 759789 / 1	Experiment ID : 1107NS88	Test Type : 08	Units : Molar
Report Date : November 29, 2011	Test Date : July 25, 2011	QNS :	MC :
COMI : 105624	Stain Reagent : SRB Dual-Pass Related	SSPL : 0XXS	

			Log10 Concentration												
	Time		Mean Optical Densities					Percent Growth							
Panel/Cell Line	Zero	Ctrl	-8.0	-7.0	-6.0	-5.0	-4.0	-8.0	-7.0	-6.0	-5.0	-4.0	GI50	TGI	LC50
Leukemia															
CCRF-CEM	0.549	1.969	1.890	1.817	1.568	1.376	1.732	94	89	72	58	83	> 1.00E-4	> 1.00E-4	> 1.00E-4
HL-60(TB)	0.902	2.535	2.644	2.627	1.811	1.398	1.768	107	106	56	30	53	.	> 1.00E-4	> 1.00E-4
MOLT-4	0.646	1.975	2.031	2.122	1.651	1.391	1.793	104	111	76	56	86	> 1.00E-4	> 1.00E-4	> 1.00E-4
RPMI-8226	0.767	1.870	1.887	1.874	1.595	1.371	1.578	101	100	75	55	73	> 1.00E-4	> 1.00E-4	> 1.00E-4
SR	0.562	1.752	1.733	1.740	0.792	0.712	0.824	98	99	19	13	22	4.12E-7	> 1.00E-4	> 1.00E-4
Non-Small Cell Lung Cancer															
A549/ATCC	0.305	1.413	1.450	1.505	1.230	0.788	1.065	103	108	83	44	69	.	> 1.00E-4	> 1.00E-4
EKVX	0.801	1.712	1.647	1.615	1.363	1.154	1.281	93	89	62	39	53	.	> 1.00E-4	> 1.00E-4
HOP-62	0.358	0.956	1.010	0.945	0.753	0.590	0.415	109	98	66	39	10	3.86E-6	> 1.00E-4	> 1.00E-4
NCI-H226	0.638	1.841	1.768	1.749	1.590	1.334	1.421	94	92	79	58	65	> 1.00E-4	> 1.00E-4	> 1.00E-4
NCI-H322M	0.823	1.557	1.537	1.593	1.491	1.312	1.326	97	105	91	67	69	> 1.00E-4	> 1.00E-4	> 1.00E-4
NCI-H460	0.212	1.817	1.850	1.859	1.510	0.569	1.024	102	103	81	22	51	.	> 1.00E-4	> 1.00E-4
NCI-H522	0.371	1.089	0.984	0.982	0.643	0.569	0.616	85	85	38	28	34	5.52E-7	> 1.00E-4	> 1.00E-4
Colon Cancer															
COLO 205	0.248	0.781	0.816	0.846	0.683	0.510	0.588	107	112	82	49	64	.	> 1.00E-4	> 1.00E-4
HCC-2998	0.544	1.898	1.858	1.768	1.489	1.260	1.386	97	90	70	53	62	> 1.00E-4	> 1.00E-4	> 1.00E-4
HCT-116	0.189	1.391	1.410	1.426	0.985	0.447	0.779	102	103	66	21	49	2.30E-6	> 1.00E-4	> 1.00E-4
HCT-15	0.286	1.597	1.526	1.572	0.918	0.585	0.817	95	98	48	23	40	9.20E-7	> 1.00E-4	> 1.00E-4
HT29	0.157	1.006	0.989	0.941	0.491	0.245	0.491	98	92	39	10	39	6.29E-7	> 1.00E-4	> 1.00E-4
KM12	0.468	2.261	2.288	2.318	1.452	0.997	1.335	101	103	55	30	48	1.55E-6	> 1.00E-4	> 1.00E-4
SW-620	0.188	1.209	1.175	1.149	0.688	0.408	0.644	97	94	49	22	45	9.49E-7	> 1.00E-4	> 1.00E-4
CNS Cancer															
SF-268	0.476	1.488	1.429	1.487	1.273	1.126	0.818	94	100	79	64	34	2.93E-5	> 1.00E-4	> 1.00E-4
SF-295	0.712	1.988	1.876	1.834	1.272	0.903	0.888	91	88	44	15	14	7.25E-7	> 1.00E-4	> 1.00E-4
SF-539	0.698	1.767	1.757	1.732	1.509	1.309	1.217	99	97	76	57	48	6.68E-5	> 1.00E-4	> 1.00E-4
SNB-19	0.542	1.330	1.284	1.227	1.022	0.910	0.779	94	87	61	47	30	5.83E-6	> 1.00E-4	> 1.00E-4
SNB-75	0.962	1.743	1.587	1.436	1.365	1.244	1.213	80	61	52	36	32	1.26E-6	> 1.00E-4	> 1.00E-4
U251	0.313	1.313	1.288	1.365	1.110	0.945	0.619	97	105	80	63	31	2.54E-5	> 1.00E-4	> 1.00E-4
Melanoma															
LOX IMVI	0.281	2.074	1.965	1.942	1.385	0.687	1.299	94	93	62	23	57	.	> 1.00E-4	> 1.00E-4
MALME-3M	0.616	0.987	0.994	0.999	0.829	0.784	0.814	102	103	57	45	53	.	> 1.00E-4	> 1.00E-4
M14	0.386	1.270	1.322	1.310	0.898	0.760	0.856	106	104	58	42	53	.	> 1.00E-4	> 1.00E-4
MDA-MB-435	0.455	1.843	1.769	1.650	0.419	0.338	0.411	95	86	-8	-26	-10	2.42E-7	8.22E-7	> 1.00E-4
SK-MEL-2	0.471	0.879	0.856	0.875	0.746	0.666	0.687	94	99	67	48	53	.	> 1.00E-4	> 1.00E-4
SK-MEL-28	0.493	1.259	1.215	1.194	0.996	0.841	0.918	94	92	66	45	55	.	> 1.00E-4	> 1.00E-4
SK-MEL-5	0.383	2.102	2.021	1.963	1.517	0.948	1.406	95	92	66	33	60	.	> 1.00E-4	> 1.00E-4
UACC-257	0.909	1.801	1.808	1.793	1.651	1.532	1.563	101	99	83	70	73	> 1.00E-4	> 1.00E-4	> 1.00E-4
UACC-62	0.782	2.373	2.243	2.135	1.605	1.149	1.368	92	85	52	23	37	1.15E-6	> 1.00E-4	> 1.00E-4
Ovarian Cancer															
IGROV1	0.531	1.211	1.259	1.262	0.959	0.817	0.757	107	108	63	42	33	4.16E-6	> 1.00E-4	> 1.00E-4
OVCAR-3	0.426	1.259	1.264	1.323	1.027	0.861	0.977	101	108	72	52	66	> 1.00E-4	> 1.00E-4	> 1.00E-4
OVCAR-4	0.417	0.964	0.948	0.903	0.807	0.720	0.837	97	89	71	55	77	> 1.00E-4	> 1.00E-4	> 1.00E-4
OVCAR-5	0.507	1.122	1.081	1.161	0.993	0.908	0.989	93	106	79	65	78	> 1.00E-4	> 1.00E-4	> 1.00E-4
OVCAR-8	0.404	1.539	1.576	1.598	1.409	1.162	0.913	103	105	89	67	45	5.79E-5	> 1.00E-4	> 1.00E-4
NCI/ADR-RES	0.526	1.792	1.763	1.700	1.028	0.800	1.109	98	93	40	22	46	6.39E-7	> 1.00E-4	> 1.00E-4
SK-OV-3	0.533	1.077	1.083	1.097	1.026	0.790	0.824	101	104	91	47	54	.	> 1.00E-4	> 1.00E-4
Renal Cancer															
786-0	0.720	2.127	2.089	2.084	1.866	1.514	1.567	97	97	81	56	60	> 1.00E-4	> 1.00E-4	> 1.00E-4
A498	1.180	1.702	1.573	1.534	1.455	1.172	1.494	75	68	53	-1	60	.	.	> 1.00E-4
ACHN	0.380	1.350	1.323	1.396	1.197	0.955	0.853	97	105	84	59	49	7.66E-5	> 1.00E-4	> 1.00E-4
CAKI-1	0.789	2.003	1.914	1.797	1.264	1.121	1.305	93	83	39	27	42	5.64E-7	> 1.00E-4	> 1.00E-4
RXF 393	0.515	1.091	1.057	1.005	0.815	0.668	0.654	94	85	52	27	24	1.20E-6	> 1.00E-4	> 1.00E-4
SN12C	0.506	1.519	1.398	1.374	1.166	0.873	1.031	88	86	65	36	52	.	> 1.00E-4	> 1.00E-4
TK-10	0.466	1.034	1.058	1.003	0.931	0.871	0.877	104	94	82	71	72	> 1.00E-4	> 1.00E-4	> 1.00E-4
UO-31	0.697	1.380	1.312	1.363	1.194	1.032	1.245	90	97	73	49	80	.	> 1.00E-4	> 1.00E-4
Prostate Cancer															
PC-3	0.461	1.583	1.605	1.514	1.227	1.016	1.094	102	94	68	49	56	.	> 1.00E-4	> 1.00E-4
DU-145	0.442	1.539	1.579	1.556	1.469	1.261	1.159	104	102	94	75	65	> 1.00E-4	> 1.00E-4	> 1.00E-4
Breast Cancer															
MCF7	0.393	1.815	1.671	1.704	1.142	0.659	1.051	90	92	53	19	46	1.20E-6	> 1.00E-4	> 1.00E-4
MDA-MB-231/ATCC	0.571	1.116	1.036	1.031	0.772	0.692	0.535	85	84	37	22	-6	5.28E-7	5.98E-5	> 1.00E-4
HS 578T	0.810	1.762	1.684	1.642	1.418	1.193	1.065	92	87	64	40	27	3.84E-6	> 1.00E-4	> 1.00E-4
BT-549	0.736	1.489	1.471	1.480	1.209	1.086	1.283	98	99	63	46	73	.	> 1.00E-4	> 1.00E-4
T-47D	0.591	1.381	1.333	1.346	1.186	1.069	0.957	94	96	75	60	46	5.48E-5	> 1.00E-4	> 1.00E-4
MDA-MB-468	0.513	1.323	1.229	1.175	0.680	0.588	0.735	88	82	21	9	27	3.30E-7	> 1.00E-4	> 1.00E-4

Fig. 9. Five dose assay of compound **4a** (NSC: 105624/759789).

ligands using OPLS 2005 force field. The low energy conformation of the ligands was selected and was docked into the grid generated from protein structures using standard precision (SP) docking mode. The final evaluation is done with glide score (docking score) and single best pose is generated as the output for particular ligand.

7. Results and discussion

7.1. Pharmacophore modeling

The pharmacophore mapping was carried out to map the chemical features or functional groups present in the synthesized compounds which are essential for anticancer activity. We generated different pharmacophore pattern based on a set of synthesized aligned molecules. Selected pharmacophore shows five chemical features which were present in all the synthesized molecules (indicated by 100%) as shown in Fig. 5. The information shows that the five features used were two AroC feature (Aromatic), AliC feature (Aliphatic) one HDr (Hydrogen bond donor) features. The average RMSD of the pharmacophore alignment of each two molecule is 0.010511 Å. These five chemical features were found in all the synthesized molecules. The larger tessellated spheres are indicative of the common pharmacophore identified in the molecule. The smaller solid features are of the individual molecules. The common pharmacophore having four larger orange color tessellated sphere shows aromatic and aliphatic carbon. Magneta color larger tessellated sphere shows the hydrogen bond donor as shown in Fig. 5. The distance among the various chemical features are as follows;

1. AroS (Benzothiazole) to AroC (Aniline) = 4.872 Å
2. AroS (Benzothiazole) to AliC (1st methyl of aniline) = 4.202 Å
3. AroS (Benzothiazole) to HDr (−NH−) = 5.392 Å
4. AroC (Aniline) to HDr (−NH−) = 5.351 Å
5. AroC (Aniline) to AliC (1st methyl of aniline) = 3.275 Å
6. HDr (−NH−) to AliC (1st methyl of aniline) = 3.621 Å
7. HDr (−NH−) to AliC (6th methyl of aniline) = 4.872 Å

Hypothesis generation was performed using low energy conformers of the molecules. All adapted models showed that the donor atoms of the NH fragments (magenta color larger tessellated) as hydrophilic element and the aryl moieties as hydrophobic element were well superimposed within the set distance tolerance. This confirms the important role of the hydrophilic and hydrophobic moieties for recognition and binding to receptor sites.

According to the pharmacophore generated by Molsign the minimal structural requirements for antitumor activity consist of an aromatic ring (hydrophobic region) attached to NH fragment (H-bonding donor region), and a hydrophobic region represented

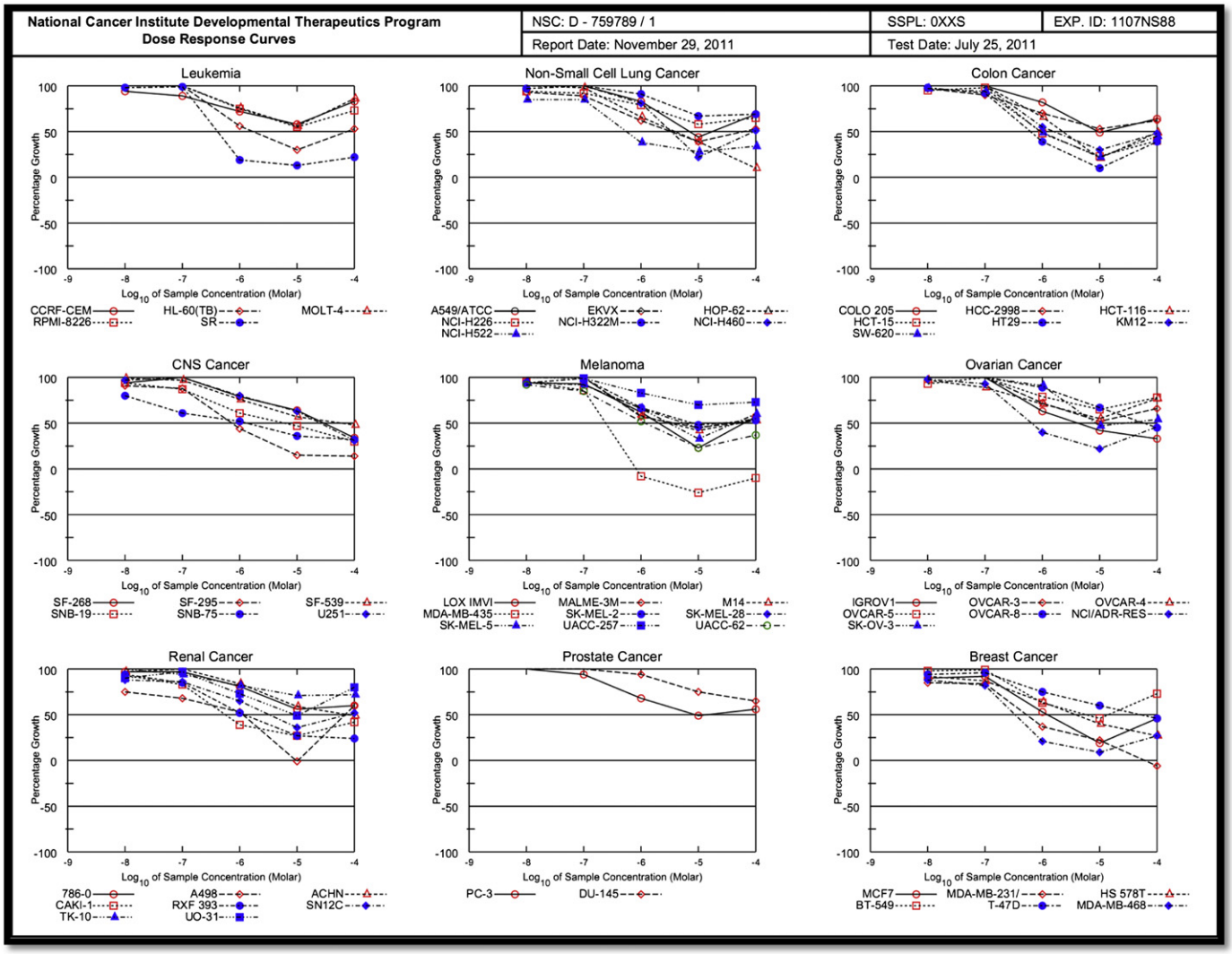

Fig. 10. Five dose assay graph of compound **4a** (NSC: 105624/759789) against nine panel cancer cell line at NCI.

by benzothiazole core. This pharmacophoric assumption was in consistence with biological data.

7.2. Docking study

Docking study was carried out for the target compounds into EGFR using GLIDE (Schordinger Inc., USA) (2006). The crystal structure of the enzyme with lapatinib (1XKK) was obtained from protein data bank PDB [40]. Since it was found that gefitinib mimic ATP and bind to the ATP binding region of the kinase active site. Our compounds were modeled by positioning them in the lapatinib binding site in accordance with the published crystal structures of quinazoline derivatives bound to kinase [42]. The entire complex was then subjected to alternate cycles of minimization and dynamics. The intent was to get a satisfactory structure for the complex that was consistent with the published crystal structure [43,44]. From the comparative docking study of our compounds with many structurally related lead compounds such as lapatinib and gefitinib we could observe how our compounds might bind to the kinase binding site, based on the knowledge of the structure of similar active sites. We redocked lapatinib into the active site of the enzyme and then we replaced with our compounds in order to compare the binding mode of both ligand and the test compound. These docking studies have revealed that the benzothiazole ring binds to a narrow hydrophobic pocket in the N-terminal domain of EGFR TK where N- of the benzothiazole ring interacts with the backbone NH of Met-793 via a hydrogen bond. These interactions underscore the importance of both nitrogen atoms for binding and the subsequent inhibitory capacity. The aniline moiety at C-2 of benzothiazole lies in a deep and hydrophobic pocket similar to the 3′-chloro-4′-(3-fluorobenzyl)oxy moiety of lapatinib. The results of this virtual screening could support the postulation that our active compounds may act on the same enzyme target where EGFR inhibitor acts.

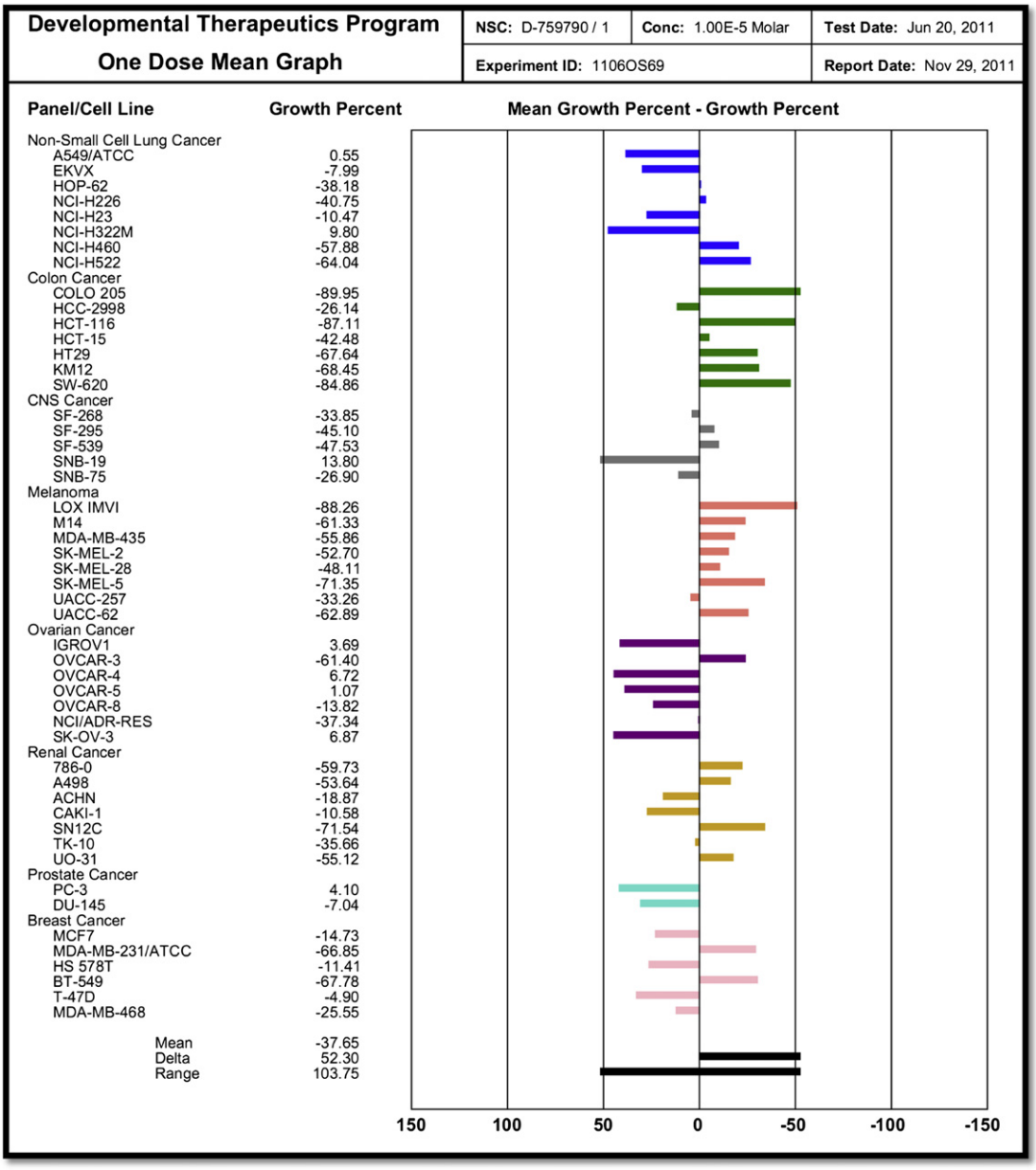

Fig. 11. Single dose assay of compound **4i** (NSC: 105628/759390).

Figs. 6 and 7 demonstrate binding mode of lapatinib and benzothiazoles (**4i**) in the ATP binding site. Lapatinib forms hydrogen bonding with MET-793 via N-1 of quinazoline and similar hydrogen bonding interaction is also shown by N-3 of benzothiazoles (**4i**) with MET-793 and in case of compound **4e** and **4j**, we noticed additional H bond between N of nitro group and H atom of amino acid backbone of ASP-855. Residues within 5 Å areas of lapatinib and benzothiazoles (**4i**) are shown in Fig. 7. Some

National Cancer Institute Developmental Therapeutics Program
In-Vitro Testing Results

NSC : D - 759790 / 1	Experiment ID : 1107NS88	Test Type : 08	Units : Molar
Report Date : November 29, 2011	Test Date : July 25, 2011	QNS :	MC :
COMI : 105628	Stain Reagent : SRB Dual-Pass Related	SSPL : 0XXS	

		Log10 Concentration												
	Time	Mean Optical Densities						Percent Growth						
Panel/Cell Line	Zero	Ctrl	-8.0	-7.0	-6.0	-5.0	-4.0	-8.0	-7.0	-6.0	-5.0	-4.0	GI50	TGI	LC50
Leukemia															
CCRF-CEM	0.549	1.929	1.869	1.839	1.399	0.364	0.483	96	93	62	-34	-12	1.32E-6	4.43E-6	> 1.00E-4
HL-60(TB)	0.902	2.580	2.652	2.637	1.964	0.479	0.390	104	103	63	-47	-57	1.32E-6	3.75E-6	2.06E-5
MOLT-4	0.646	1.880	1.966	1.986	1.285	0.398	0.495	107	109	52	-38	-23	1.05E-6	3.75E-6	> 1.00E-4
RPMI-8226	0.767	1.819	1.848	1.786	1.249	0.619	0.667	103	97	46	-19	-13	8.29E-7	5.05E-6	> 1.00E-4
SR	0.562	1.793	1.793	1.802	1.193	0.286	0.383	100	101	51	-49	-32	1.03E-6	3.24E-6	> 1.00E-4
Non-Small Cell Lung Cancer															
A549/ATCC	0.305	1.509	1.539	1.497	0.970	0.106	0.137	103	99	55	-65	-55	1.11E-6	2.87E-6	7.47E-6
EKVX	0.801	1.646	1.612	1.490	0.931	0.092	0.215	96	82	15	-89	-73	2.99E-7	1.40E-6	4.26E-6
HOP-62	0.358	1.114	1.141	1.087	0.863	0.025	0.091	104	96	67	-93	-75	1.27E-6	2.62E-6	5.38E-6
HOP-92	1.089	1.388	1.329	1.224	0.995	0.187	0.307	80	45	-9	-83	-72	7.18E-8	6.90E-7	3.61E-6
NCI-H226	0.638	1.842	1.779	1.639	1.352	0.188	0.266	95	83	59	-71	-58	1.18E-6	2.86E-6	6.95E-6
NCI-H322M	0.823	1.619	1.559	1.635	1.432	0.138	0.043	92	102	76	-83	-95	1.46E-6	3.01E-6	6.19E-6
NCI-H460	0.212	1.965	2.001	1.887	1.390	0.054	0.130	102	96	67	-75	-39	1.32E-6	2.97E-6	.
NCI-H522	0.371	1.154	1.063	1.042	0.770	0.107	0.189	88	86	51	-71	-49	1.02E-6	2.61E-6	.
Colon Cancer															
COLO 205	0.248	0.916	0.951	0.875	0.741	0.024	0.119	105	94	74	-91	-52	1.40E-6	2.81E-6	5.67E-6
HCC-2998	0.544	1.577	1.495	1.445	1.271	0.064	0.195	92	87	70	-88	-64	1.34E-6	2.78E-6	5.74E-6
HCT-116	0.189	1.443	1.494	1.436	0.825	0.004	0.051	104	99	51	-98	-73	1.01E-6	2.19E-6	4.75E-6
HCT-15	0.286	1.656	1.564	1.644	1.101	0.042	0.075	93	99	59	-85	-74	1.16E-6	2.57E-6	5.69E-6
HT29	0.157	1.089	1.088	1.056	0.762	0.045	0.070	100	96	65	-71	-56	1.29E-6	2.99E-6	6.97E-6
KM12	0.468	2.131	2.123	2.145	1.504	0.021	0.010	99	101	62	-96	-98	1.20E-6	2.48E-6	5.15E-6
SW-620	0.188	1.305	1.273	1.202	0.955	0.027	0.034	97	91	69	-86	-82	1.32E-6	2.78E-6	5.86E-6
CNS Cancer															
SF-268	0.476	1.579	1.561	1.545	1.158	0.064	0.211	98	97	62	-87	-56	1.20E-6	2.61E-6	5.66E-6
SF-295	0.712	2.094	1.997	1.851	1.174	0.096	0.348	93	82	33	-87	-51	4.59E-7	1.90E-6	4.96E-6
SF-539	0.698	1.845	1.814	1.843	1.582	0.136	0.303	97	100	77	-81	-57	1.48E-6	3.08E-6	6.40E-6
SNB-19	0.542	1.498	1.413	1.399	1.191	0.139	0.201	91	90	68	-74	-63	1.34E-6	3.00E-6	6.74E-6
SNB-75	0.962	1.883	1.720	1.747	1.386	0.654	0.996	82	85	46	-32	4	7.91E-7	.	> 1.00E-4
U251	0.313	1.332	1.373	1.316	1.004	0.050	0.158	104	98	68	-84	-50	1.31E-6	2.79E-6	.
Melanoma															
LOX IMVI	0.281	1.976	1.881	1.783	1.221	0.047	0.222	94	89	55	-83	-21	1.09E-6	2.51E-6	.
MALME-3M	0.616	1.033	1.035	0.991	0.832	0.098	0.098	101	90	52	-84	-84	1.03E-6	2.40E-6	5.60E-6
M14	0.386	1.293	1.324	1.298	1.048	0.123	0.169	103	101	73	-68	-56	1.46E-6	3.29E-6	7.44E-6
MDA-MB-435	0.455	1.935	1.874	1.744	1.141	0.105	0.149	96	87	46	-77	-67	8.13E-7	2.38E-6	6.05E-6
SK-MEL-2	0.471	0.953	0.941	0.893	0.814	0.169	0.265	98	88	71	-64	-44	1.43E-6	3.35E-6	.
SK-MEL-28	0.493	1.299	1.243	1.253	1.111	0.070	0.155	93	94	77	-86	-69	1.46E-6	2.96E-6	6.02E-6
SK-MEL-5	0.383	2.102	2.004	1.930	1.247	0.021	0.092	94	90	50	-95	-76	1.00E-6	2.22E-6	4.93E-6
UACC-257	0.909	1.865	1.881	1.873	1.563	0.266	0.298	102	101	68	-71	-67	1.35E-6	3.10E-6	7.09E-6
UACC-62	0.782	2.492	2.381	2.246	1.651	0.120	0.051	94	86	51	-85	-94	1.01E-6	2.37E-6	5.55E-6
Ovarian Cancer															
IGROV1	0.531	1.260	1.362	1.279	0.936	0.238	0.242	114	103	55	-55	-55	1.12E-6	3.17E-6	8.96E-6
OVCAR-3	0.426	1.328	1.305	1.299	0.874	0.019	0.101	98	97	50	-96	-76	9.83E-7	2.20E-6	4.86E-6
OVCAR-4	0.417	0.999	0.964	0.899	0.675	0.043	0.053	94	83	44	-90	-87	7.08E-7	2.14E-6	5.05E-6
OVCAR-5	0.507	1.116	1.128	1.068	0.991	0.034	0.018	102	92	79	-93	-96	1.48E-6	2.88E-6	5.61E-6
OVCAR-8	0.404	1.649	1.664	1.659	1.126	0.119	0.264	101	101	58	-71	-35	1.15E-6	2.83E-6	.
NCI/ADR-RES	0.526	1.674	1.664	1.524	0.939	0.146	0.239	99	87	36	-72	-55	5.31E-7	2.15E-6	6.23E-6
SK-OV-3	0.533	1.132	1.135	1.129	1.046	0.057	-0.036	101	99	86	-89	-100	1.60E-6	3.08E-6	5.95E-6
Renal Cancer															
786-0	0.720	2.175	2.265	2.081	1.475	0.048	0.074	106	94	52	-93	-90	1.03E-6	2.28E-6	5.03E-6
A498	1.180	1.789	1.697	1.589	1.337	0.040	0.092	85	67	26	-97	-92	2.60E-7	1.62E-6	4.16E-6
ACHN	0.380	1.318	1.305	1.296	0.939	0.005	-0.024	99	98	60	-99	-100	1.15E-6	2.38E-6	4.92E-6
CAKI-1	0.789	2.006	1.910	1.672	1.008	0.075	0.199	92	73	18	-90	-75	2.59E-7	1.46E-6	4.23E-6
RXF 393	0.515	1.140	1.102	0.973	0.798	0.137	0.311	94	73	45	-73	-40	6.76E-7	2.41E-6	.
SN12C	0.506	1.550	1.452	1.389	0.983	0.031	0.081	91	85	46	-94	-84	7.72E-7	2.12E-6	4.85E-6
TK-10	0.466	1.079	1.064	1.042	0.831	0.067	0.155	98	94	59	-86	-67	1.16E-6	2.57E-6	5.67E-6
UO-31	0.697	1.424	1.337	1.106	0.886	0.061	0.268	88	56	26	-91	-62	1.61E-7	1.67E-6	4.44E-6
Prostate Cancer															
PC-3	0.461	1.568	1.524	1.353	0.884	0.149	0.121	96	81	38	-68	-74	5.26E-7	2.30E-6	6.81E-6
DU-145	0.442	1.591	1.657	1.613	1.309	0.018	0.066	106	102	75	-96	-85	1.41E-6	2.75E-6	5.39E-6
Breast Cancer															
MCF7	0.393	1.798	1.661	1.609	1.044	0.057	0.178	90	87	46	-86	-55	8.11E-7	2.24E-6	5.37E-6
MDA-MB-231/ATCC	0.571	1.154	1.109	1.045	0.668	0.042	0.171	92	81	17	-93	-70	3.04E-7	1.42E-6	4.06E-6
HS 578T	0.810	1.913	1.774	1.705	1.352	0.475	0.669	87	81	49	-41	-17	9.38E-7	3.49E-6	> 1.00E-4
BT-549	0.736	1.476	1.493	1.487	1.323	0.100	0.380	102	101	79	-86	-48	1.50E-6	3.01E-6	.
T-47D	0.591	1.401	1.364	1.413	0.962	0.060	0.215	95	102	46	-90	-64	8.41E-7	2.18E-6	5.08E-6
MDA-MB-468	0.513	1.289	1.201	1.142	0.691	0.140	0.212	89	81	23	-73	-59	3.43E-7	1.74E-6	5.79E-6

Fig. 12. Five dose assay of compound **4i** (NSC: 105628/759390).

common residues involved in this type of interaction within 5 Å area are ALA-743, ARG-841, ASP-855, CYS-797, LEU-718, LEU-777, LEU-788, LYS-745, MET-766, THR-790 and THR-854 as shown in Table 2.

7.3. Primary single high dose (10^{-5} M) full NCI 60 cell panel in vitro assay

The tumor growth inhibition properties of the two compounds **4a** and **4i** with the NCI codes 105624/759789 and 105628/759390 selected among **4(a–j)** by the National Cancer Institute (NCI), USA, were screened on human tumor cell lines at single high dose (10^{-5} M) and five dose level at the NIH, Bethesda, Maryland, USA, under the drug discovery program of the NCI.

With regard to sensitivity against individual cell lines at primary single high dose (10^{-5} M). Compound **4a** showed remarkably lowest cell growth promotion against CNS cancer SNB-75 cell line and Melanoma MDA-MB-435 cancer cell line with cell growth promotion of −15.50 and −23.68 respectively as shown in Fig. 8. On the other hand compound **4i** was found to be broad spectrum against all nine panel of cancer cell line at primary single high dose (10^{-5} M) as shown in Fig. 11.

7.4. In vitro 5 dose full NCI 60 cell panel assay

All the cell lines (about 60), representing nine tumor subpanels, were incubated at five different concentrations (0.01, 0.1, 1, 10 & 100 μM). The outcomes were used to create log concentration Vs % growth inhibition curves and three response parameters (GI_{50}, TGI and LC_{50}) were calculated for each cell line. The GI_{50} value (growth inhibitory activity) corresponds to the concentration of the compound causing 50% decrease in net cell growth, the TGI value (cytostatic activity) is the concentration of the compound resulting in total growth inhibition and LC_{50} value (cytotoxic activity) is the concentration of the compound causing net 50% loss of initial cells at the end of the incubation period of 48 h [34–36].

Compound under investigation **4a** exhibited remarkable anti-cancer activity against most of the tested cell lines representing nine different subpanels with GI_{50} value 4.12×10^{-7} M against Leukemia SR cell line, 5.52×10^{-7} M against Non-Small Cell Lung Cancer NCI-H5222 cell line, 9.20×10^{-7} M, 6.29×10^{-7} M, 9.47×10^{-7} M against Colon Cancer HCT-116, HCT-15and SW-620 cancer cell line respectively, 7.25×10^{-7} M against CNS cancer SF-295 cancer cell line, 2.42×10^{-7} M against Melanoma MDA-MB-435 cancer cell line, 6.39×10^{-7} M against Ovarian NCI/ADR-RES cancer cell line, 5.64×10^{-7} M against Renal Cancer CAKI-1

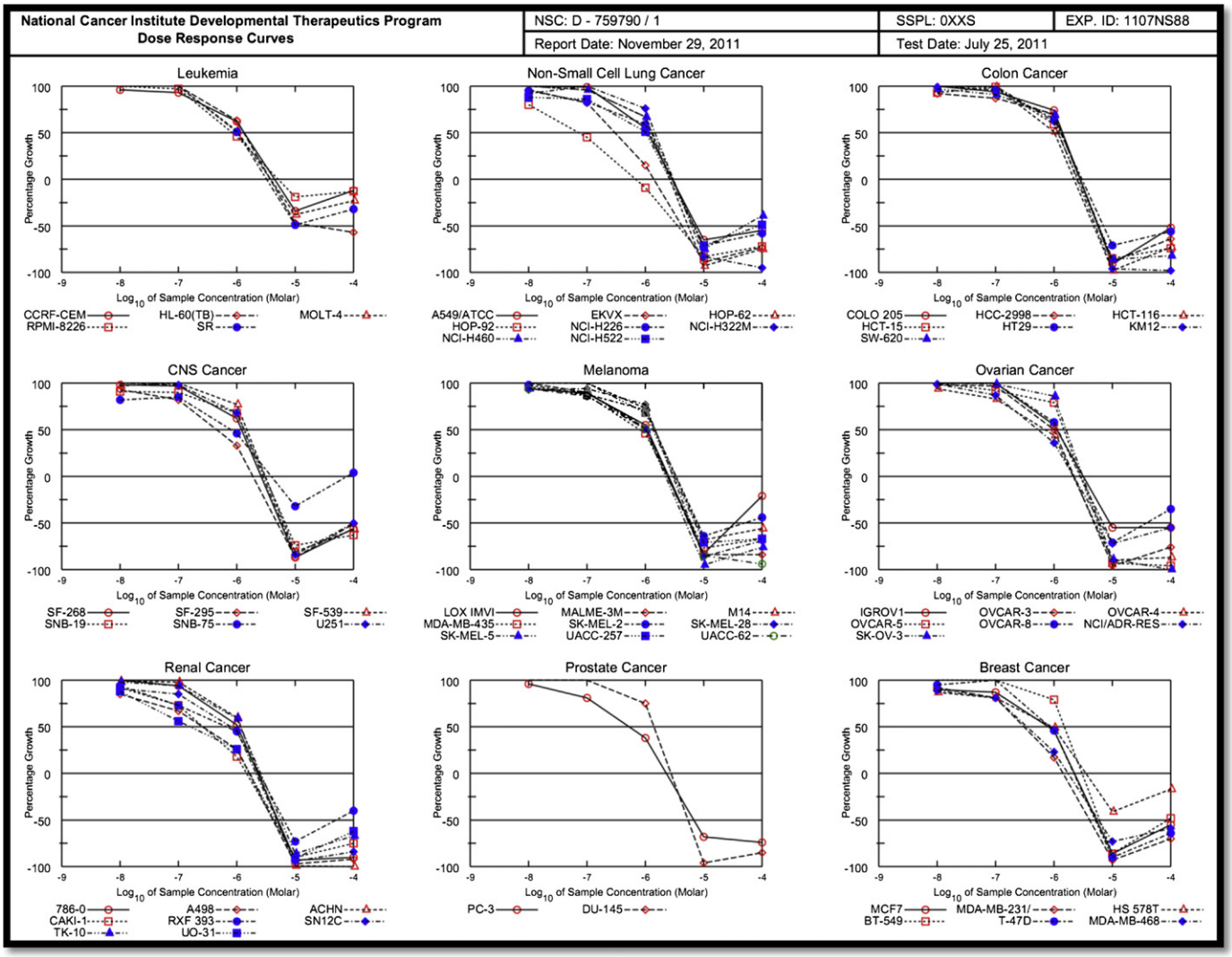

Fig. 13. Five dose assay graph of compound **4i** (NSC: 105628/759390) against nine panel of cancer cell line at NCI.

cancer cell line, 5.28×10^{-7} M and 3.30×10^{-7} M against Breast MDA-MB-231/ATCC and MDA-MB-468 cancer cell line. A sign of ">" is used as prefix to the concentration for those cell lines which were found to be insensitive at the highest tested concentration i.e. 100 μM as shown in Figs. 9 and 10.

With regard to the sensitivity against some individual cell lines the compound **4i** showed highest activity against Non-Small Cell HOP-92 Lung cancer cell line with GI_{50} value of 7.18×10^{-8} M. Obtained data revealed an obvious broad spectrum sensitivity profile of **4i** toward all 9 subpanel of cancer cell line with GI_{50} value ranging from 1.60×10^{-6} M to 7.18×10^{-8} M, least for Non-Small Cell HOP-92 Lung cancer and maximum for OVCAR-SK-OV-3 cell line as shown in Figs. 12 and 13.

On the basis of results obtained it was found that compound **4i** (NSC: 105628/759390) was most active compound of the series. Based on close examination on substitutions, it may be concluded that the role of electron withdrawing groups (−Cl) has great influence on anticancer activity, it is also proved by the docking study where compound **4a** is having dock score of −7.85 kcal/mol and **4i** is having −9.95 kcal/mol. Finally it is conceivable that further derivatization of such compounds will be of interest with the hope to get more selective anticancer agents.

8. Conclusion

Compounds 7-chloro-*N*-(2,6-dichlorophenyl)benzo[*d*]thiazol-2-amine (**4a**) with GI_{50} values of 7.18×10^{-8} M against Non-Small Cell Lung Cancer HOP-92 cancer cell line proved to be the most active members in this study. This benzothiazole analog could be considered as useful templates for future development to obtain more potent antitumor agent(s). Flexible alignment was conducted on the basis of experimental data from which five featured pharmacophore model was developed. This pharmacophore model could be very useful for the virtual screening in the development of new antitumor agents. According to the pharmacophore generated by Molsign the minimal structural requirements for antitumor activity consist of an aromatic ring (hydrophobic region) attached to NH fragment (H-bonding donor region), and a hydrophobic region represented by benzothiazole core. Molecular docking studies further supports our assumption that the synthesized compounds have analogous binding mode to the EGFR inhibitors and demonstrates the various interactions between the ligands and enzyme active sites and thereby help to design novel potent inhibitors. The overall outcome of this model revealed that: (i) the benzothiazole ring is a satisfactory backbone for antitumor activity, (ii) the presence of substituted aniline moiety at the C-2 amino position is necessary for the activity as hydrophobic region, (iii) the presence of electron withdrawing group on benzothiazole ring and on substituted aniline at 2nd position enhances the anticancer activity. (iv) secondary amino group at 2nd position of benzothiazoles is acting as conformational lock and extending substituted aniline portion into the hydrophobic pockets of EGFR-tyrosine kinase, making predominantly hydrophobic interactions with the protein mimicking the 3′-chloro-4′-[(3-fluorobenzyl)oxy] aniline group of lapatinib. These preliminary encouraging results of biological screening of the tested compounds could offer an excellent framework in this field that may lead to discovery of potent antitumor agent.

9. Experimental

All chemicals and solvents were supplied by Merck, S.D. Fine Chemical Limited, Mumbai. All the solvents were distilled and dried before use. The reactions were monitored with the help of thin-layer chromatography using pre-coated aluminum sheets with GF_{254} silica gel, 0.2 mm layer thickness (E. Merck). Melting points of the synthesized compounds were recorded on the Veego (VMP-MP) melting point apparatus. IR spectrum was acquired on a Shimadzu Infra Red Spectrometer, (model FTIR-8400S). Both ^{1}H-NMR (DMSO) and ^{13}C NMR (DMSO) spectra of the synthesized compounds were performed with Bruker Avance-II 400 NMR Spectrometer operating at 400 MHz in SAIF, Punjab University (Chandigarh). Chemical shifts were measured relative to internal standard TMS (δ:0). Chemical shifts are reported in δ scale (ppm). Mass spectra of the synthesized compounds were recorded at MAT 120 in SAIF, Punjab University.

9.1. Synthesis of substituted isothiocyanates **2(a–e)** [33]

9.1.1. Synthesis of substituted thioureas **3(a–j)** [25]

*9.1.1.1. General procedure for the synthesis of substituted 2-amino benzothiazoles **4(a–j)**.* Substituted thioureas **3 (a–j)** (0.01 mol) were dissolved in chloroform (15 ml), the reaction mixture was cooled in an ice bath and then bromine: chloroform (1:9) mixture was added drop wise. The reaction was monitored by TLC and after an hour, was poured on to crushed ice. The solid that separated was filtered, dried in each case and then purified by column chromatography using silica gel. It was eluted with $CHCl_3$: EtOAc (7:3) and the eluents on evaporation and crystallization yielded pure solid substituted 2-amino benzothiazoles.

*9.1.1.1.1. N-(2,6-dimethylphenyl)-6-methylbenzo[d]thiazol-2-amine (**4a**).* This compound was prepared and purified as per the above mentioned procedure; IR (KBr) υ_{max} 3301 (NH-strech), 3039 (Arom. CH strech), 2937 (Aliph. CH strech), 1602 (NH-bend) cm^{-1}; ^{1}H NMR (DMSO-d_6) δ ppm: 7.46–8.33 (m, 6H, Ar–H), 4.54 (s, 1H, NH), 2.32 (s, 6H, CH_3), 2.46 (s, 3H, CH_3); ^{13}C NMR (DMSO-d_6) δ ppm:172.3, 154.3, 138.7, 134.2, 130.7, 124.2, 120.6, 21.6 (benzothiazole), 140.2, 138.2, 131.3, 124.6, 20.2 (2,6-dimethyl aniline); HRMS (EI) *m/z* calcd for $C_{16}H_{16}N_2S$: 268.1034; found: 268.1038.

*9.1.1.1.2. 6-bromo-N-(2,6-dimethylphenyl)benzo[d]thiazol-2-amine (**4b**).* This compound was prepared and purified as per the above mentioned procedure; IR (KBr) υ_{max} 3256 (NH-strech), 3049 (Arom. CH strech), 2919 (Aliph. CH strech), 1563 (NH-bend), 623 (C–Br) cm^{-1}; ^{1}H NMR (DMSO-d_6) δ ppm: 6.76–7.35 (m, 6H, Ar–H), 4.26 (s, 1H, NH), 1.99 (s, 6H, CH_3); ^{13}C NMR (DMSO-d_6) δ ppm: 173.1, 156.2, 134.2, 130.1, 126.3, 120.8, 118.6 (benzothiazole), 141.8, 138.6, 130.3, 125.5, 21.3 (2,6-dimethyl aniline); HRMS (EI) *m/z* calcd for $C_{15}H_{13}BrN_2S$: 331.9983; found: 331.9981.

*9.1.1.1.3. N-(2,6-dimethylphenyl)-6-nitrobenzo[d]thiazol-2-amine (**4c**).* This compound was prepared and purified as per the above mentioned procedure; IR (KBr) υ_{max} 3379 (NH-strech), 3118 (Arom. CH strech), 2952 (Aliph. CH strech), 1583 (NH-bend),1552,1349 (NO_2) cm^{-1}; ^{1}H NMR (DMSO-d_6) δ ppm: 6.98–7.85 (m, 6H, Ar–H), 4.54 (s, 1H, NH), 2.23 (s, 6H, CH_3); ^{13}C NMR (DMSO-d_6) δ ppm: 174.8, 162.3, 149.2, 134.4, 126.4, 122.2, 119.2 (benzothiazole), 139.6, 136.2, 130.2, 126.2, 20.4 (2,6-dimethyl aniline); HRMS (EI) *m/z* calcd for: $C_{15}H_{13}N_3O_2S$: 299.0728; found: 299.0732.

*9.1.1.1.4. 7-chloro-N-(2,6-dimethylphenyl)benzo[d]thiazol-2-amine (**4d**).* This compound was prepared and purified as per the above mentioned procedure; IR (KBr) υ_{max} 3391 (NH-strech), 3134 (Arom. CH strech), 2817 (Aliph. CH strech), 1584 (NH-bend), 727 (C–Cl) cm^{-1}; ^{1}H NMR (DMSO-d_6) δ ppm: 6.85–8.17 (m, 6H, Ar–H), 5.47 (s, 1H, NH), 2.20 (s, 6H, CH_3); ^{13}C NMR (DMSO-d_6) δ ppm: 171.3, 154.2, 136.3, 134.2, 132.1, 130.6, 118.2 (benzothiazole), 141.2, 139.4, 131.3, 125.1, 20.3 (2,6-dimethyl aniline); HRMS (EI) *m/z* calcd for $C_{15}H_{13}ClN_2S$: 288.0488; found: 288.0492.

*9.1.1.1.5. N-(2,6-dimethylphenyl)-7-nitrobenzo[d]thiazol-2-amine (**4e**) [45].* This compound was prepared and purified as per the above mentioned procedure; IR (KBr) υ_{max} 3291 (NH-strech), 3051 (Arom. CH strech), 2962 (Aliph. CH strech), 1574 (NH-bend),

1548,1354 (NO_2) cm^{-1}; ^1H NMR (DMSO-d_6) δ ppm: 6.76–8.14 (m, 6H, Ar–H), 4.23 (s, 1H, NH), 2.28 (s, 6H, CH_3); ^{13}C NMR (DMSO-d_6) δ ppm: 171.3, 152.3, 146.2, 132.8, 131.4, 128.4, 122.3 (benzothiazole), 140.2, 136.4, 132.6, 124.9, 20.8 (2,6-dimethyl aniline); HRMS (EI) *m/z* calcd for $C_{15}H_{13}N_3O_2S$: 299.0728; found: 299.0724.

*9.1.1.1.6. N-(2,6-dichlorophenyl)-6-methylbenzo[d]thiazol-2-amine (**4f**).* This compound was prepared and purified as per the above mentioned procedure; IR (KBr) υ_{max} 3312 (NH-strech), 3061 (Arom. CH strech), 2923 (Aliph. CH strech), 1589 (NH-bend), 684 (C–Cl) cm^{-1}; ^1H NMR (DMSO-d_6) δ ppm: 6.81–8.10 (m, 6H, Ar–H), 4.21 (s, 1H, NH), 2.21 (s, 3H, CH_3); ^{13}C NMR (DMSO-d_6) δ ppm: 173.4, 152.4, 136.5, 132.6, 128.4, 124.4, 118.4, 21.3 (benzothiazole), 140.2, 137.2, 130.3, 122.6 (2,6-dichloro aniline); HRMS (EI) *m/z* calcd for$C_{14}H_{10}C_{l2}N_2S$: 307.9942; found: 307.9945.

*9.1.1.1.7. 6-bromo-N-(2,6-dichlorophenyl)benzo[d]thiazol-2-amine (**4g**).* This compound was prepared and purified as per the above mentioned procedure; IR (KBr) υ_{max} 3331 (NH-strech), 3012 (CH strech), 1591 (NH-bend), 711 (C–Cl), 623 (C–Br) cm^{-1}; ^1H NMR (DMSO-d_6) δ ppm: 6.76–7.33 (m, 6H, Ar–H), 4.36 (s, 1H, NH); ^{13}C NMR (DMSO-d_6) δ ppm: 171.3, 156.2, 134.8, 130.2, 125.1, 122.6, 118.3 (benzothiazole), 139.2, 138.6, 129.8, 124.6 (2,6-dichloro aniline); HRMS (EI) *m/z* calcd for $C_{13}H_7BrCl_2N_2S$: 371.8890; found: 371.8895.

*9.1.1.1.8. N-(2,6-dichlorophenyl)-6-nitrobenzo[d]thiazol-2-amine (**4h**).* This compound was prepared and purified as per the above mentioned procedure; IR (KBr) υ_{max} 3308 (NH-strech), 3008 (CH strech), 1594 (NH-bend), 1552,1346 (NO_2), 725 (C–Cl) cm^{-1}; ^1H NMR (DMSO-d_6) δ ppm: 6.88–8.23 (m, 6H, Ar–H), 4.01 (s, 1H, NH); ^{13}C NMR (DMSO-d_6) δ ppm: 170.3, 162.9, 146.4, 134.8, 124.6, 120.2, 118.5 (benzothiazole), 141.3, 138.5, 129.8, 121.3 (2,6-dichloro aniline); HRMS (EI) *m/z* calcd for $C_{13}H_7Cl_2N_3O_2S$: 338.9636; found: 338.9641.

*9.1.1.1.9. 7-chloro-N-(2,6-dichlorophenyl)benzo[d]thiazol-2-amine (**4i**).* This compound was prepared and purified as per the above mentioned procedure; IR (KBr) υ_{max} 3256 (NH-strech), 3112 (CH strech), 1576 (NH-bend), 761 (C–Cl), cm^{-1}; ^1H NMR (DMSO-d_6) δ ppm: 6.72–8.10 (m, 6H, Ar–H), 4.51 (s, 1H, NH); ^{13}C NMR (DMSO-d_6) δ ppm: 172.4, 152.4, 132.4, 130.2, 128.4, 125.4, 121.3 (benzothiazole), 140.7, 138.4, 128.2, 120.6 (2,6-dichloro aniline); HRMS (EI) *m/z* calcd for$C_{13}H_7Cl_3N_2S$: 327.9396; found: 327.9391.

*9.1.1.1.10. N-(2,6-dichlorophenyl)-7-nitrobenzo[d]thiazol-2-amine (**4j**).* This compound was prepared and purified as per the above mentioned procedure; IR (KBr) υ_{max} 3323 (NH-strech), 3075 (CH strech), 1584 (NH-bend),1555, 1351 (NO_2) 703 (C–Cl) cm^{-1}; ^1H NMR (DMSO-d_6) δ ppm: 7.12–7.94 (m, 6H, Ar–H), 4.52 (s, 1H, NH); ^{13}C NMR (DMSO-d_6) δ ppm: 173.5, 152.3, 146.2, 136.2, 135.8, 125.6, 120.3 (benzothiazole), 142.3, 139.5, 131.6, 121.7 (2,6-dichloro aniline); HRMS (EI) *m/z* calcd for $C_{13}H_7Cl_2N_3O_2S$: 338.9636; found: 338.9632.

Acknowledgment

The authors would like to thank Director General, Department of Science and Technology, Government of India, New Delhi, for funding the project (Grant No. SR/FT/LS-0024/2008).

References

[1] E. Zwick, J. Bange, A. Ullrich, Endocr. Relat. Cancer 8 (2001) 161–173.
[2] W.J. Gullick, Br. Med. Bull. 47 (1991) 87–98.
[3] Y. Yardern, A. Ullrich, Annu. Rev. Biochem 57 (1988) 443–478.
[4] K. Yamazaki, Y. Kaneko, K. Suwa, S. Ebara, K. Nakazawa, K. Yasuno, Bioorg. Med. Chem. 13 (2005) 2509–2522.
[5] E. Brantley, S. Antony, G. Kohlhagen, L.H. Meng, K. Agama, S.F. Stinson, E.A. Sausville, Y. Pommier, Cancer Chemother. Pharmacol. 58 (2006) 62–72.
[6] C.J. Lion, C.S. Matthews, G. Wells, T.D. Bradshaw, M.F.G. Stevens, A.D. Westwell, Bioorg. Med. Chem. Lett. 16 (2006) 5005–5008.
[7] S.T. Huang, I.J. Hsei, C. Chen, Bioorg. Med. Chem. 14 (2006) 6106–6119.
[8] M. Yoshida, I. Hayakawa, N. Hayashi, T. Agatsuma, Y. Oda, F. Tanzawa, S. Iwasaki, K. Koyama, H. Furukawa, S. Kurakata, Y. Sugano, Bioorg. Med. Chem. Lett. 15 (2005) 3328–3332.
[9] J. Das, R.V. Moquin, J. Lin, C. Liu, A.M. Doweyko, H.F. DeFex, Q. Fang, S. Pang, S. Pitt, D.R. Shen, G.L. Schieven, J.C. Barrish, J. Wityak, Bioorg. Med. Chem. Lett. 13 (2003) 2587–2590.
[10] S.E. O'Brien, H.L. Browne, T.D. Bradshaw, A.D. Westwell, M.F.G. Stevens, C.A. Laughton, Org. Biomol. Chem. 1 (2003) 493–497.
[11] I. Hutchinson, S.A. Jennings, B.R. Vishnuvajjala, A.D. Westwell, M.F.G. Stevens, J. Med. Chem. 45 (2002) 744–747.
[12] S. Saeed, N. Rashid, P.G. Jones, M. Ali, R. Hussain, Eur. J. Med. Chem. 45 (2010) 1323–1331.
[13] H.S.A. Elzahabi, Eur. J. Med. Chem. 46 (2011) 4025–4036.
[14] W.P. Hu, Y.K. Chen, C.C. Liao, H.S. Yu, Y.M. Tsai, S.M. Huang, F.Y. Tsai, H.C. Shen, L.S. Chang, J.J. Wang, Bioorg. Med. Chem. 46 (2010) 6197–6207.
[15] G.M. Catriona, W. Geoffrey, C.P. Jean, L.S. Erica, D.B. Tracey, F.G.S. Malcolm, D.W. Andrew, J. Med. Chem. 49 (2006) 179–185.
[16] Y.A. Al-Soud, Arkivoc 15 (2008) 225–238.
[17] E. Kashiyama, I. Hutchinson, M.S. Chua, S.F. Stinson, L.R. Phillips, G. Kaur, E.A. Sausville, T.D. Bradshaw, A.D. Westwell, M.F.G. Stevens, J. Med. Chem. 42 (1999) 4172–4184.
[18] T.D. Bradshaw, S. Wrigley, D.F. Shi, R.J. Schultz, K.D. Paull, M.F.G. Stevens, Br. J. Cancer 77 (1998) 745–752.
[19] M.F.G. Stevens, C.J. McCall, P. Lelieveld, P. Alexander, A. Richter, D.E. Davies, J. Med. Chem. 37 (1994) 1689–1695.
[20] P.C. Yates, C.J. McCall, M.F.G. Stevens, Tetrahedron 47 (1991) 6493–6502.
[21] T. Akiyama, J. Ishida, S. Nakagawa, H. Ogawara, S. Watenabe, N. Itoh, M. Shibuya, Y. Fukami, J. Biol. Chem. 262 (1987) 5592–5595.
[22] Y. Graziani, E. Erikson, R.L. Erikson, Eur. J. Biochem. 135 (1983) 583–589.
[23] M. Cushman, D. Nagrathnam, D.L. Burg, R.L. Geahlem, J. Med. Chem. 34 (1991) 798–806.
[24] B.D.M. Cunningham, M.D. Threadgill, P.W. Groundwater, I.L. Dale, J.A. Hickman, Anti-Cancer Drug Des 7 (1992) 365–384.
[25] S.N. Manjula, M.N. Noolvi, K.V. Parihar, S.A. Manohara Reddy, V. Ramani, A.K. Gadad, G. Singh, N.G. Kutty, M. Rao, Eur. J. Med. Chem. 44 (2009) 2923–2929.
[26] M.N. Noolvi, H.M. Patel, Eur. J. Med. Chem. 46 (2011) 2327–2346.
[27] M.N. Noolvi, H.M. Patel, Eur. J. Med. Chem. 46 (2011) 4411–4418.
[28] M.N. Noolvi, H.M. Patel, V. Bhardwaj, Med. Chem. 7 (2011) 2002.
[29] M.N. Noolvi, H.M. Patel, Lett. Drug Desi. Disc 7 (2010) 556–586.
[30] N. Hori, G. Tsukamoto, A. Imamura, M. Ohashi, T. Saito, K. Yoshino, Chem. Pharm. Bull. 40 (1992) 2387–2390.
[31] I. Hutchison, M.S. Chua, H.L. Browne, V. Trapani, T.D. Bradshaw, A.D. Westwell, M.F.G. Stevens, J. Med. Chem. 44 (2001) 1446–1455.
[32] D. Fabbro, S. Ruetz, E. Buchdunger, S.W. Cowan-Jacob, G. Fendrich, J. Liebetanz, T. O'Reilley, P. Traxler, B. Chaudhari, H. Fretz, J. Zimmermann, T. Meyer, G. Carvatti, P. Furet, P.W. Manley, Pharmacol. Ther. 93 (2002) 79–98.
[33] T. Ishikawa, J. Org. Chem. 65 (2000) 7774–7778.
[34] M.C. Alley, D.A. Scudiero, P.A. Monks, M.L. Hursey, M.J. Czerwinski, D.L. Fine, B.J. Abbott, J.G. Mayo, R.H. Shoemaker, M.R. Boyd, Cancer Res. 48 (1988) 589–601.
[35] M.R. Grever, S.A. Schepartz, B.A. Chabner, Semin. Oncol. 19 (1992) 622–638.
[36] M.R. Boyd, K.D. Paull, Drug Dev. Res. 19 (1995) 91–109.
[37] Molecular Design Suite 3.5, VLife Technologies, Pune, India. www.vlifesciences.com.
[38] T.A. Halgren, J. Comput. Chem. 17 (1996) 553–586.
[39] R.D. Cramer, D.E. Patterson, J.D. Bunce, J. Am. Chem. Soc. 110 (1988) 5959–5967.
[40] website: http://www.rcsb.org/pdb/explore.do?structureId=1XKK.
[41] H. Zhong, L.M. Tran, L. Jenna, J. Mol. Graph. Mod. 28 (2009) 336–346.
[42] L. Shewchuk, A. Hassell, B. Wisely, W. Rocque, W. Holmes, J. Veal, L.F. Kuyper, J. Med. Chem. 43 (2000) 133–138.
[43] R.W. Edgar, T.T. Anne, B.M. Octerloney, Y. Derek, H. Anne, H.D. Scott, E. Byron, P. Christopher, T.H. Earnes, L. Karen, J.A. Krystal, W.R. David, M.G. Tona, S. Lisa, Cancer Res. 64 (2004) 6652–6659.
[44] H. Assefa, S. Kamath, K. John, J. Comput. Aided Mol. Des. 17 (2003) 475–493.
[45] S. Huang, P.J. Connolly, Tetrahedron Lett. 45 (2004) 9373–9375.